

Investigating Potential Melt Sources for the Magma-Poor Albertine-Rhino Graben of the East African Rift System Using 3D Geodynamic Modeling with ASPECT

Asenath Kwagalakwe¹

¹Virginia Tech

November 21, 2022

Abstract

The leading paradigm for rift initiation suggests “magma-assisted (wet)” rifting is required to weaken strong lithosphere such that only small tectonic stresses are needed for rupture to occur. However, there is no surface expression of magma along the 300 km long Albertine-Rhino Graben (except at its southernmost tip within the Tore Ankole Volcanic Field), which is the northernmost rift in the Western Branch of the East African Rift System. The two prevailing models explaining magma-poor rifting are: 1) Melt is present at depth weakening the lithosphere, but it has not reached the surface or 2) far-field forces driving extension are accommodated along weak pre-existing structures without melt at depth. The goal of this study is to test the hypothesis that melt is generated below the Albertine-Rhino Graben from Lithospheric Modulated Convection (LMC) using the 3D finite element code ASPECT. We develop a regional model of a rigid lithosphere and an underlying convecting sublithospheric mantle that has dimensions 1000 by 1000 by 660 km along latitude, longitude, and depth, respectively. We solve the Stokes equations using the extended Boussinesq approximation for an incompressible fluid which considers the effects of adiabatic heating and frictional heating. We include latent heating such that we can test for melt generation in the sublithospheric mantle from LMC. Using LITHO1.0 as the base of our lithosphere, our preliminary results suggest melt could be generated beneath the Albertine-Rhino graben given a mantle potential temperature of 1800 K. These early results indicate LMC can generate melt beneath the northernmost Western branch of the East African Rift System.

Investigating Potential Melt Sources for the Magma-Poor Albertine-Rhino Graben of the East African Rift System Using 3D Geodynamic Modeling with ASPECT

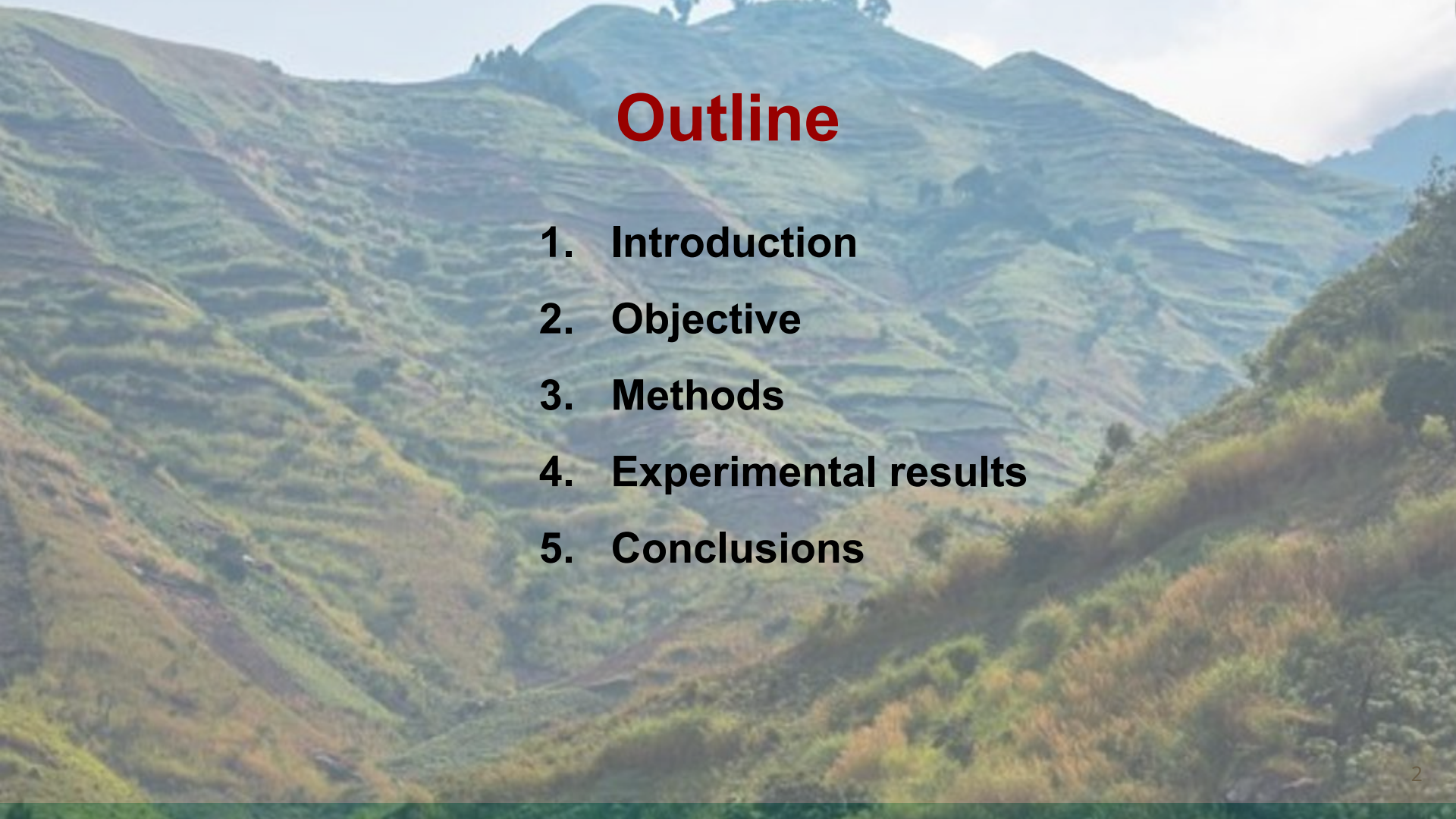
Asenath Kwagalakwe
she/her, Virginia Tech, USA

Coauthors:

D.Sarah Stamps (she/her, Virginia Tech, USA)

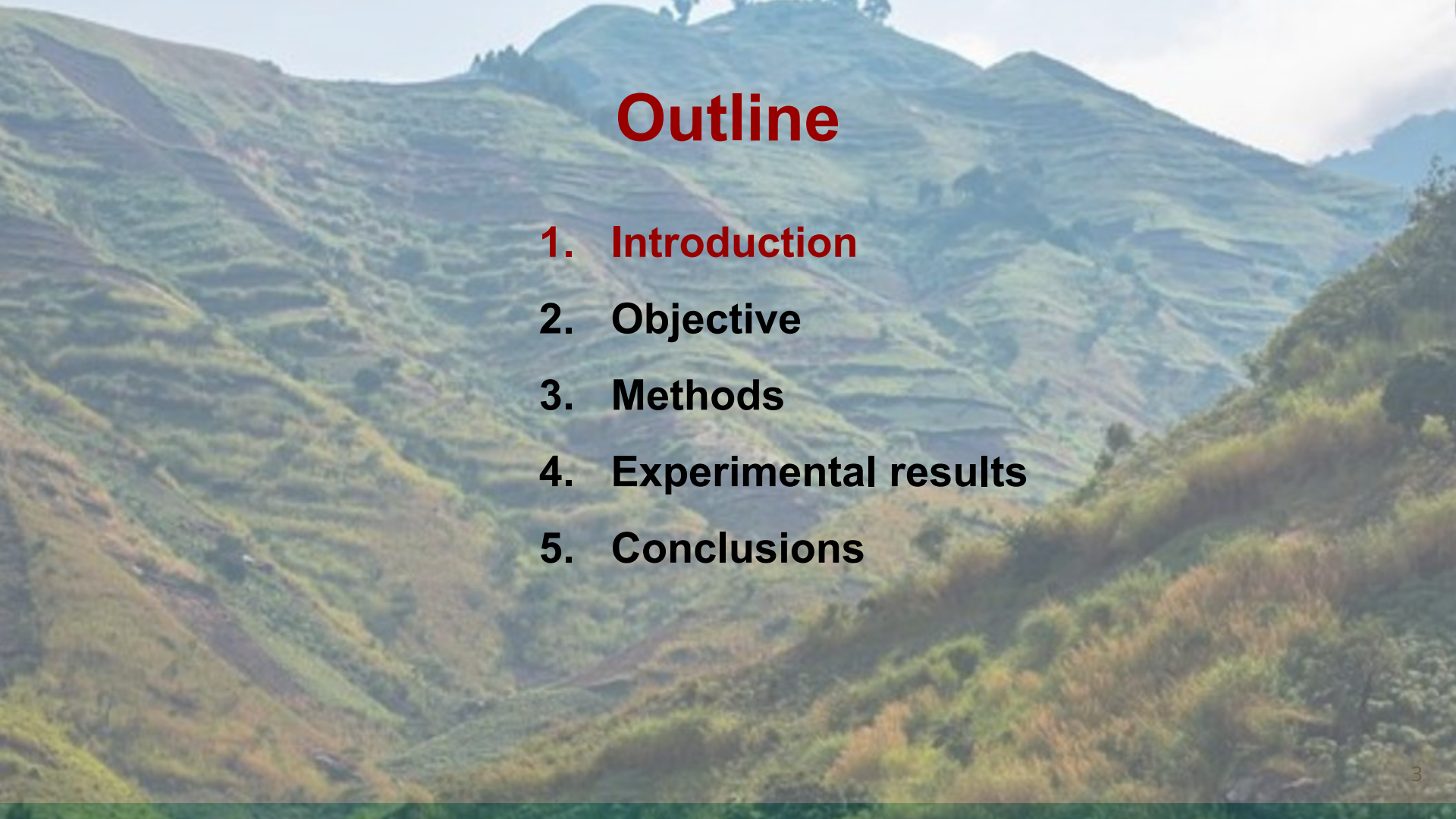
Emmanuel Njinju (he/him, Virginia Tech, USA)

Estella Atekwana (she/her, University of California, Davis, USA)

The background of the slide is a photograph of a mountain valley. The hillsides are covered in green vegetation, with visible terraced agricultural fields. A dirt road winds through the valley. The sky is blue with some light clouds.

Outline

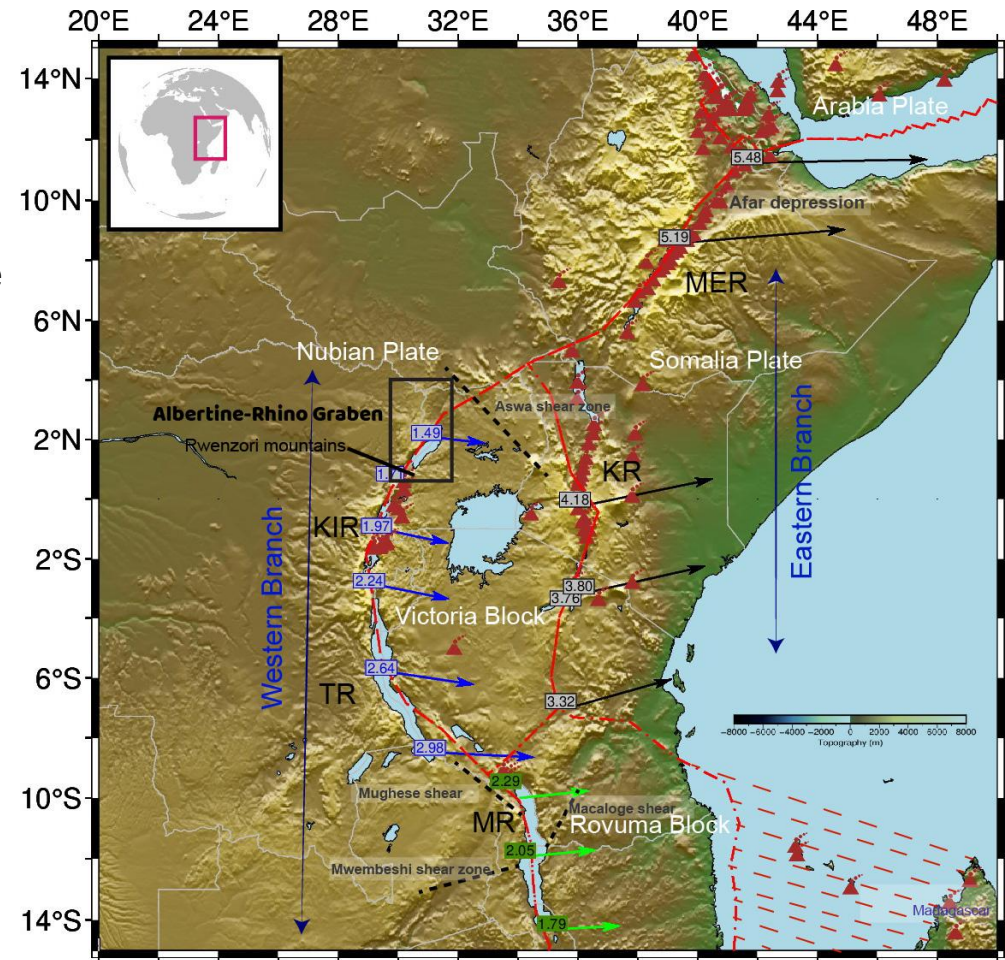
1. Introduction
2. Objective
3. Methods
4. Experimental results
5. Conclusions

A scenic view of a mountain valley with green hills and a winding road. The hills are covered in lush green vegetation, and a dirt road winds through the valley. The sky is blue with some clouds.

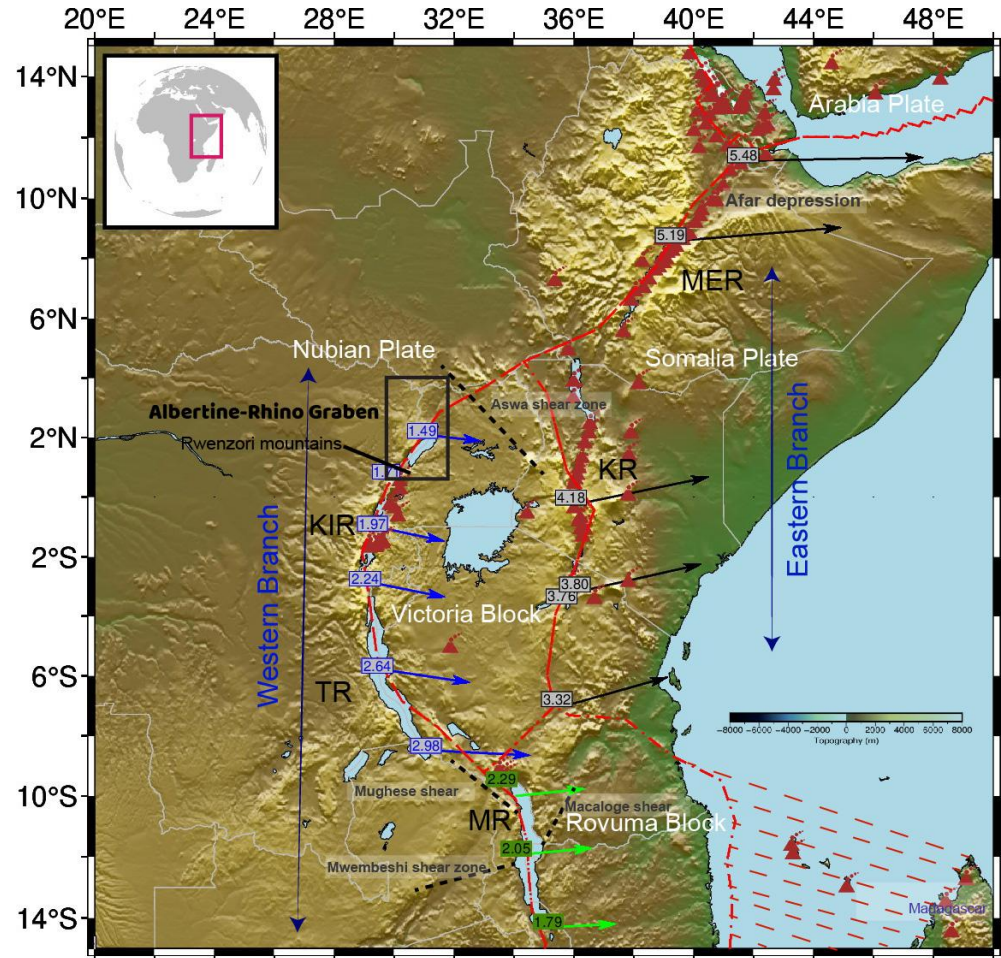
Outline

- 1. Introduction**
- 2. Objective**
- 3. Methods**
- 4. Experimental results**
- 5. Conclusions**

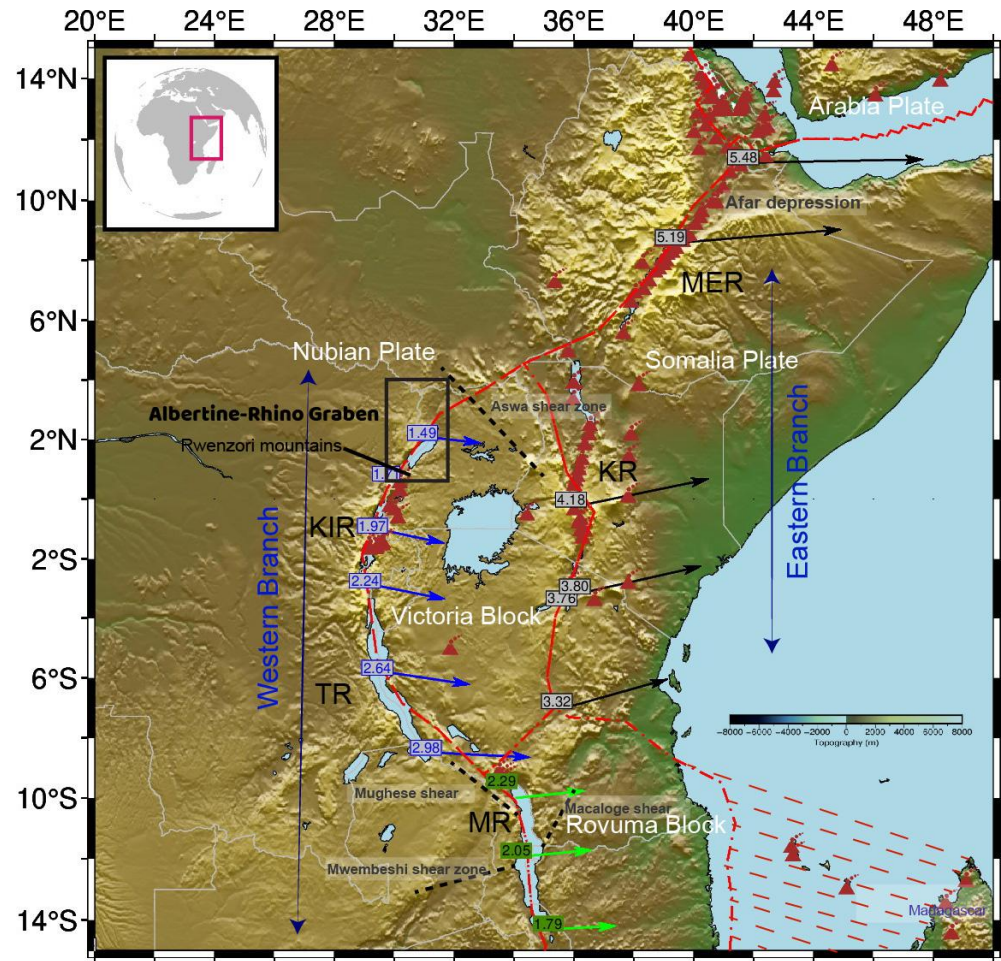
- The East African Rift (EAR) is a divergent continental setting.



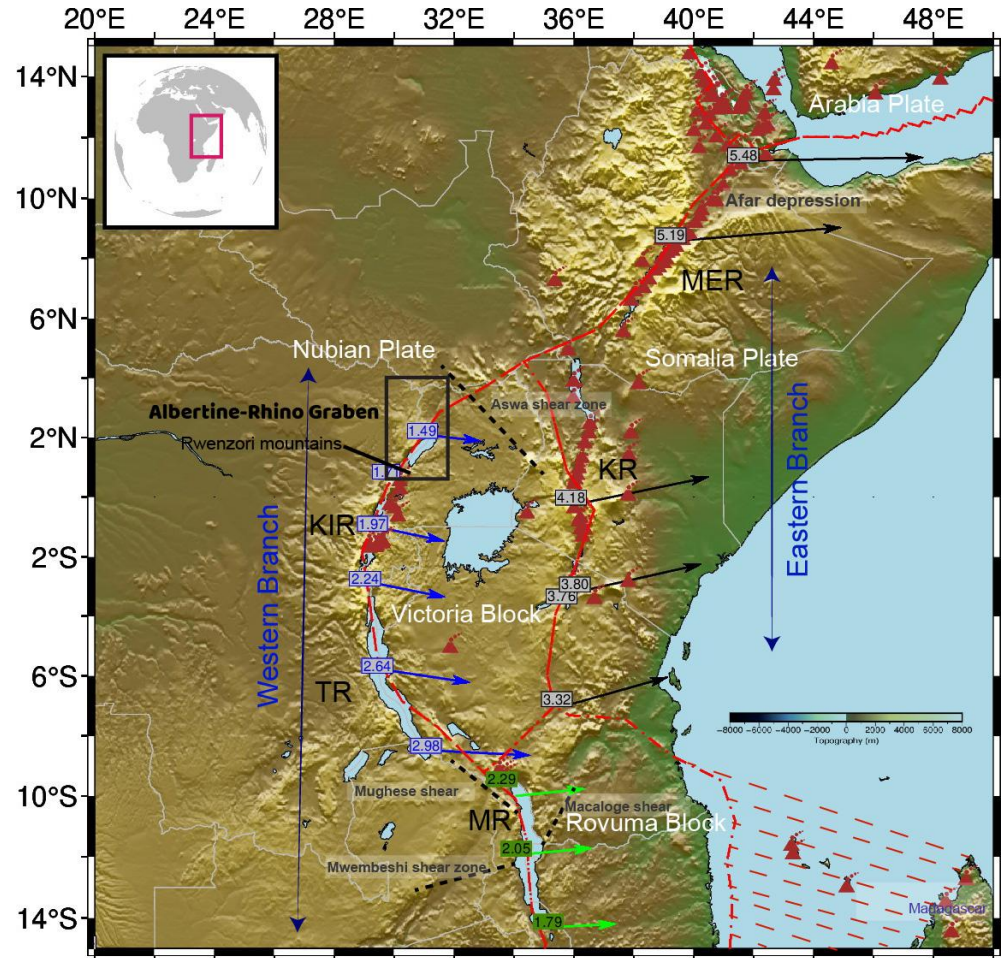
- The East African Rift (EAR) is a divergent continental setting.
- The Arabian Plate, Somalia Plate, Victoria and Rovuma Blocks are moving away from the rest of the continent (Nubian Plate)



- The East African Rift (EAR) is a divergent continental setting.
- The Arabian Plate, Somalia Plate, Victoria and Rovuma Blocks are moving away from the rest of the continent (Nubian Plate)
- The EAR has two main branches (Western and Eastern) with several rift segments



- The East African Rift (EAR) is a divergent continental setting.
- The Arabian Plate, Somalia Plate, Victoria and Rovuma Blocks are moving away from the rest of the continent (Nubian Plate)
- The EAR has two main branches (Western and Eastern) with several rift segments
- The predicted extension rates from a kinematic model constrained by GPS velocities range from 1.49 to 5.48 mm/yr (*Stamps et al., 2021*)



The amount of force required to break strong lithosphere is not always available in nature (“Tectonic Force Paradox”)

There are weakening mechanisms that facilitate rifting of strong lithosphere:

- a) Melt (Buck, 2004; Wright et al., 2006; Muirhead et al., 2016; Jones et al., 2019)
- b) Pre-existing structures (Dunbar & Sawyer, 1988; Peace et al., 2018).
- c) Fluids (Leseane et al., 2015, Muirhead et al., 2016, Weinstein et al., 2017)

The amount of force required to break strong lithosphere is not always available in nature ("Tectonic Force Paradox")

There are weakening mechanisms that facilitate rifting of strong lithosphere:

- a) Melt (Buck, 2004; Wright et al., 2006; Muirhead et al., 2016; Jones et al., 2019)
- b) Pre-existing structures (Dunbar & Sawyer, 1988; Peace et al., 2018).
- c) Fluids (Leseane et al., 2015, Muirhead et al., 2016, Weinstein et al., 2017)

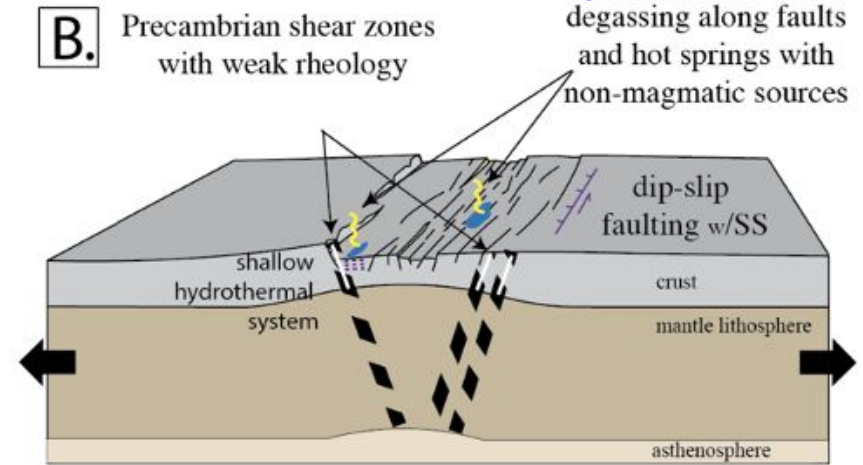
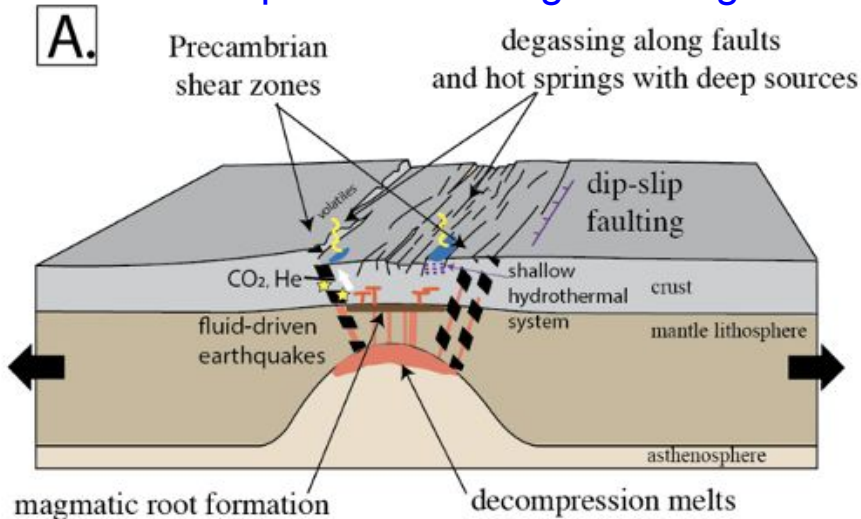
In this study, we are investigating melt as a weakening mechanism. However, there is no surface expression of magma along the 300 km Albertine-Rhino Graben (magma-poor rift)

The amount of force required to break strong lithosphere is not always available in nature ("Tectonic Force Paradox")

There are weakening mechanisms that facilitate rifting of strong lithosphere:

- Melt (Buck, 2004; Wright et al., 2006; Muirhead et al., 2016; Jones et al., 2019)
- Pre-existing structures (Dunbar & Sawyer, 1988; Peace et al., 2018).
- Fluids (Leseane et al., 2015, Muirhead et al., 2016, Weinstein et al., 2017)

In this study, we are investigating melt as a weakening mechanism. However, there is no surface expression of magma along the 300 km Albertine-Rhino Graben (magma-poor rift)

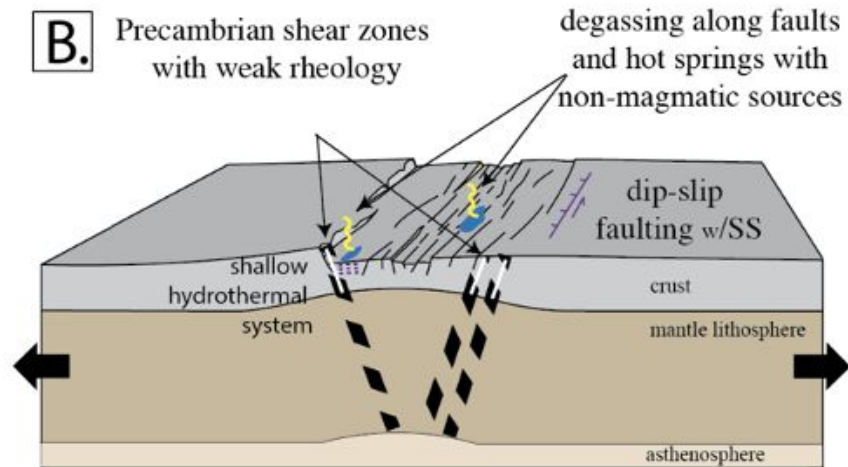
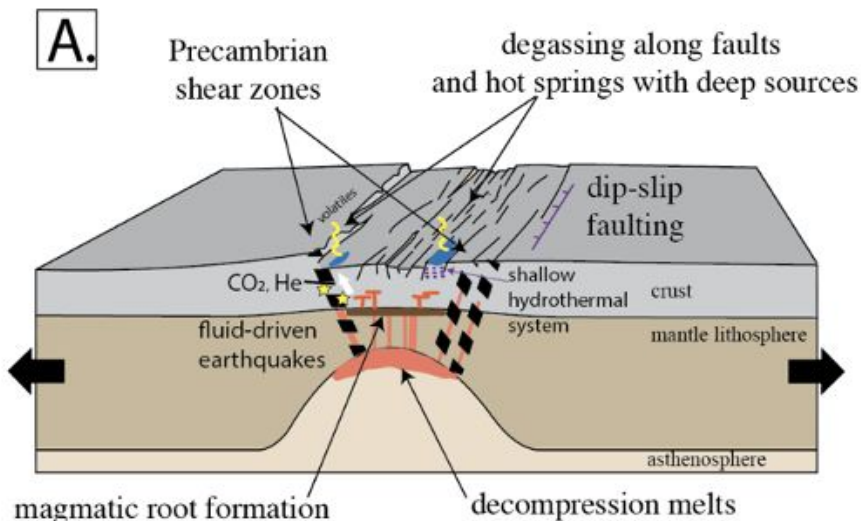


Modified from Muirhead et al., (2018, 2016).

Hypotheses we are testing for magma-poor rift segments

A: Melt is present at depth but has not reached the surface yet, and has weakened the lithosphere, allowing for strain localization during the onset of rifting.

B: Pre-existing structures or fluids weaken the lithosphere, allowing for strain localization during the onset of rifting.



Modified from Muirhead et al., (2018, 2016).

Outline

1. Introduction
2. **Objective**
3. Methods
4. Experimental results
5. Conclusions

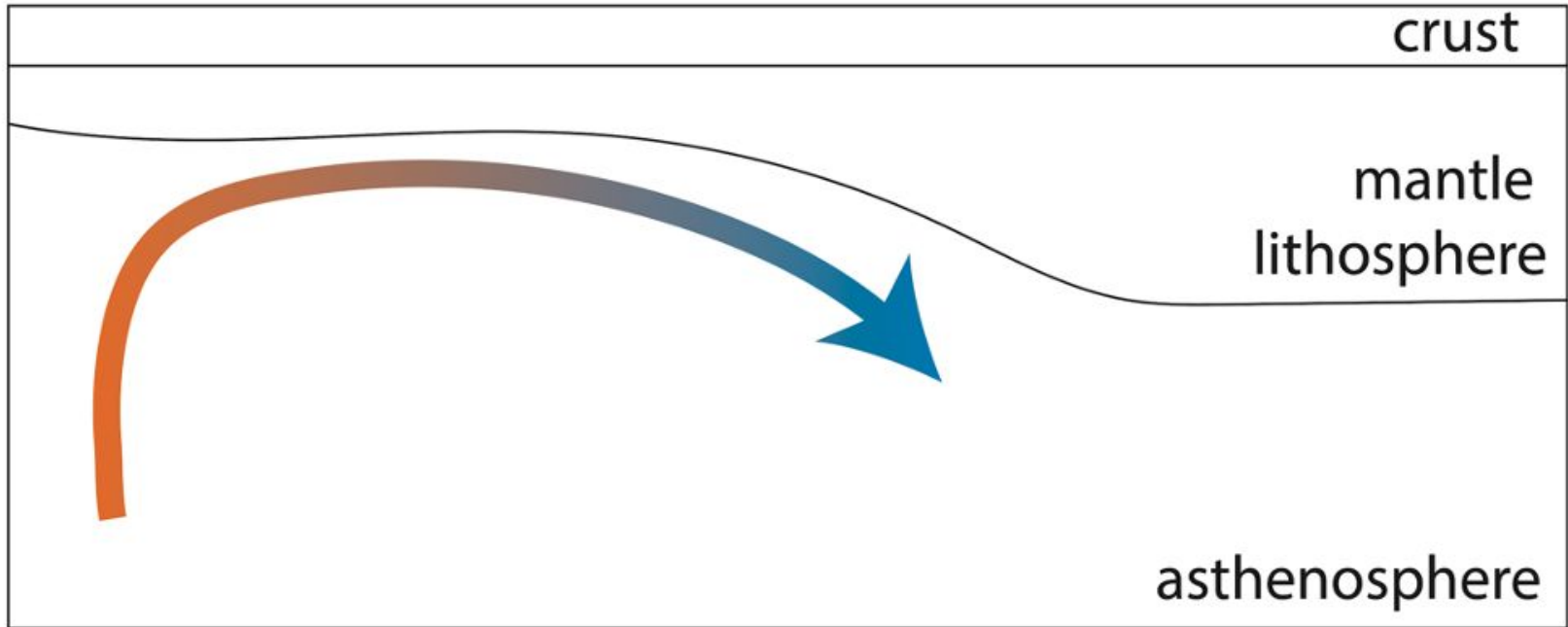
The objective of this study is to test the hypothesis that melt is present beneath the Albertine-Rhino graben, and is generated from Lithospheric Modulated Convection (LMC)

The objective of this study is to test the hypothesis that melt is present beneath the Albertine-Rhino graben, and is generated from Lithospheric Modulated Convection (LMC)

LMC is mantle convection driven by variations in lithospheric thickness that constrain the initial temperature. The base of the lithosphere (LAB) is a constant temperature below which the temperature increases adiabatically. When the lithosphere is thinner, we expect to have a hotter asthenosphere.

The objective of this study is to test the hypothesis that melt is present beneath the Albertine-Rhino graben, and is generated from Lithospheric Modulated Convection (LMC)

LMC is mantle convection driven by variations in lithospheric thickness that constrain the initial temperature. The base of the lithosphere (LAB) is a constant temperature below which the temperature increases adiabatically. When the lithosphere is thinner, we expect to have a hotter asthenosphere.



(Courtesy of D. Sarah Stamps)

Outline

1. Introduction
2. Objective
3. **Methods**
4. Experimental results
5. Conclusions

We use the CIG ASPECT (Advanced Solver for Problems in Earth's ConvecTion) code to solve the Stokes equation, the conservation of mass, and the energy equation to generate melt.

(Kronbichler et al., 2012; Bangerth et al., 2019; Dannberg and Heister, 2016)

We use the CIG ASPECT (Advanced Solver for Problems in Earth's ConvecTion) code to solve the Stokes equation, the conservation of mass, and the energy equation to generate melt.

(Kronbichler et al., 2012; Bangerth et al., 2019; Dannberg and Heister, 2016)

- a) **Conservation of Momentum** (Newton's Second Law; surface forces (Viscous & pressure forces) = body forces (buoyancy forces))

$$\underbrace{-\nabla p}_{\text{(pressure forces)}} + \underbrace{\nabla \boldsymbol{\tau}}_{\text{(Viscous forces)}} = \underbrace{\rho \mathbf{g}}_{\text{(buoyancy forces)}} \quad \text{(Stokes Equation)}$$

where $\boldsymbol{\tau}$, p , ρ , and \mathbf{g} is the shear viscosity, pressure, density, and gravitational acceleration

We use the CIG ASPECT (Advanced Solver for Problems in Earth's Convection) code to solve the Stokes equation, the conservation of mass, and the energy equation to generate melt.

(Kronbichler et al., 2012; Bangerth et al., 2019; Dannberg and Heister, 2016)

- a) **Conservation of Momentum** (Newton's Second Law; surface forces (Viscous & pressure forces) = body forces (buoyancy forces))

$$\underbrace{-\nabla p}_{\text{(pressure forces)}} + \underbrace{\nabla \boldsymbol{\tau}}_{\text{(Viscous forces)}} = \underbrace{\rho \mathbf{g}}_{\text{(buoyancy forces)}} \quad \text{(Stokes Equation)}$$

- b) **Conservation of Mass** (we assume incompressible flow where small variations of density are neglected except for the buoyancy term) $\nabla \mathbf{u} = \mathbf{0}$

where $\boldsymbol{\tau}$, p , ρ , \mathbf{g} , and \mathbf{u} is the shear viscosity, pressure, density, gravitational acceleration, and velocity

We use the CIG ASPECT (Advanced Solver for Problems in Earth's ConvecTion) code to solve the Stokes equation, the conservation of mass, and the energy equation to generate melt.

(Kronbichler et al., 2012; Bangerth et al., 2019; Dannberg and Heister, 2016)

- a) **Conservation of Momentum** (Newton's Second Law; surface forces (Viscous & pressure forces) = body forces (buoyancy forces))

$$-\nabla p \quad + \quad \nabla \tau \quad = \quad \rho g \quad (\text{Stokes Equation})$$

(pressure forces) (Viscous forces) (buoyancy forces)

- b) **Conservation of Mass** (we assume incompressible flow where small variations of density are neglected except for the buoyancy term) $\nabla \mathbf{u} = \mathbf{0}$

- c) **Conservation of Energy** (include latent heat)

$$\rho C_p [\underbrace{\partial T / \partial t + \mathbf{u} \cdot \nabla T}] \quad - \quad \kappa \nabla^2 T \quad = \quad \tau : \epsilon \quad + \quad \alpha T (\mathbf{u} \cdot \nabla p) \quad + \quad \rho T \Delta S (\partial X / \partial t + \mathbf{u} \cdot \nabla \mathbf{X})$$

(Advection) (conduction) (Frictional heating) (Adiabatic heating) (Latent heat)

where $C_p, T, \kappa, \alpha, \Delta S$, and \mathbf{X} is specific heat capacity, temperature, thermal conductivity, thermal expansivity, change in entropy, and melt fraction

We use the CIG ASPECT (Advanced Solver for Problems in Earth's Convection) code to solve the Stokes equation, the conservation of mass, and the energy equation to generate melt.

(Kronbichler et al., 2012; Bangerth et al., 2019; Dannberg and Heister, 2016)

- a) **Conservation of Momentum** (Newton's Second Law; surface forces (Viscous & pressure forces) = body forces (buoyancy forces))

$$-\nabla p \quad + \quad \nabla \tau \quad = \quad \rho g \quad (\text{Stokes Equation})$$

(pressure forces) (Viscous forces) (buoyancy forces)

- b) **Conservation of Mass** (we assume incompressible flow where small variations of density are neglected except for the buoyancy term) $\nabla \mathbf{u} = \mathbf{0}$

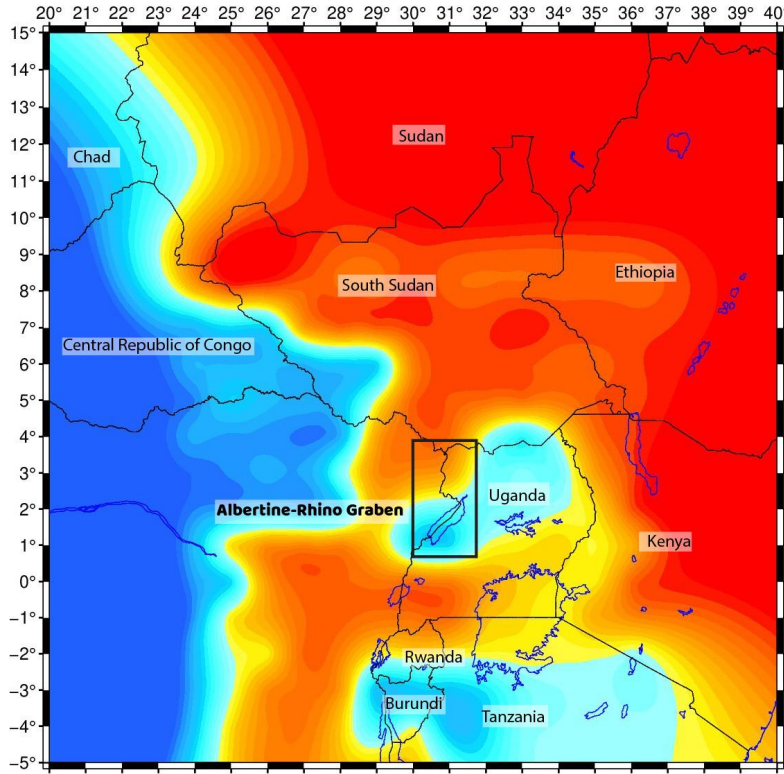
- c) **Conservation of Energy** (include latent heat)

$$\rho C_p [\underbrace{\partial T / \partial t + \mathbf{u} \cdot \nabla T}_{(\text{Advection})}] - \underbrace{\kappa \nabla^2 T}_{(\text{conduction})} = \underbrace{\tau : \epsilon}_{(\text{Frictional heating})} + \underbrace{\alpha T (\mathbf{u} \cdot \nabla p)}_{(\text{Adiabatic heat})} + \underbrace{\rho T \Delta S (\partial X / \partial t + \mathbf{u} \cdot \nabla X)}_{(\text{Latent heat})}$$

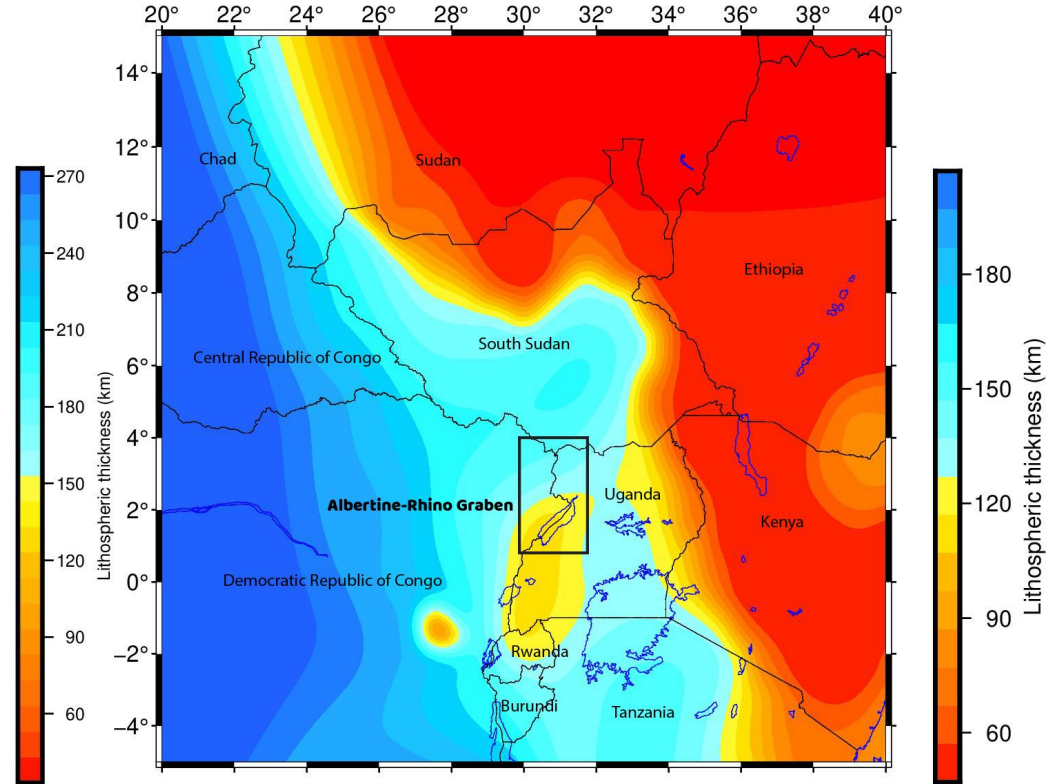
where $C_p, T, \kappa, \alpha, \Delta S$, and X is specific heat capacity, temperature, thermal conductivity, thermal expansivity, change in entropy, and melt fraction

Approximation of the governing equations: The extended Boussinesq approximation (Christensen and Yuen, 1985; Oxburgh and Turcotte, 1978). We also use the Eulerian method.

We use two seismically constrained lithospheric thickness models to constrain the initial temperature.



LITHO1.0
(Pasyanos et al., 2014)



Fishwick (2010, updated)

Model Set-up

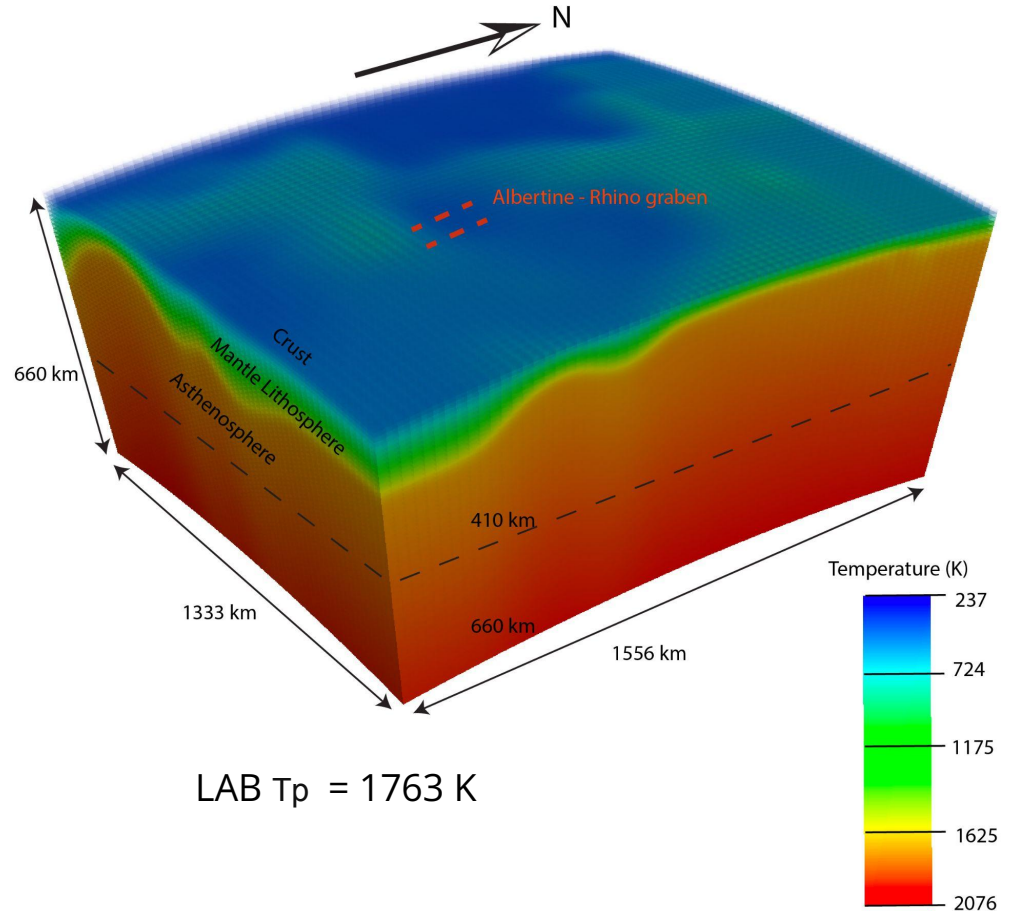
Initial temperature conditions:

Surface: 273 K

Lithosphere-Asthenosphere

Boundary (LAB): 1643, 1653, 1693, 1700, 1763K (T_p based on Rooney et al., 2012)

Below the LAB: T varies with thickness



Model Set-up

Initial density conditions:

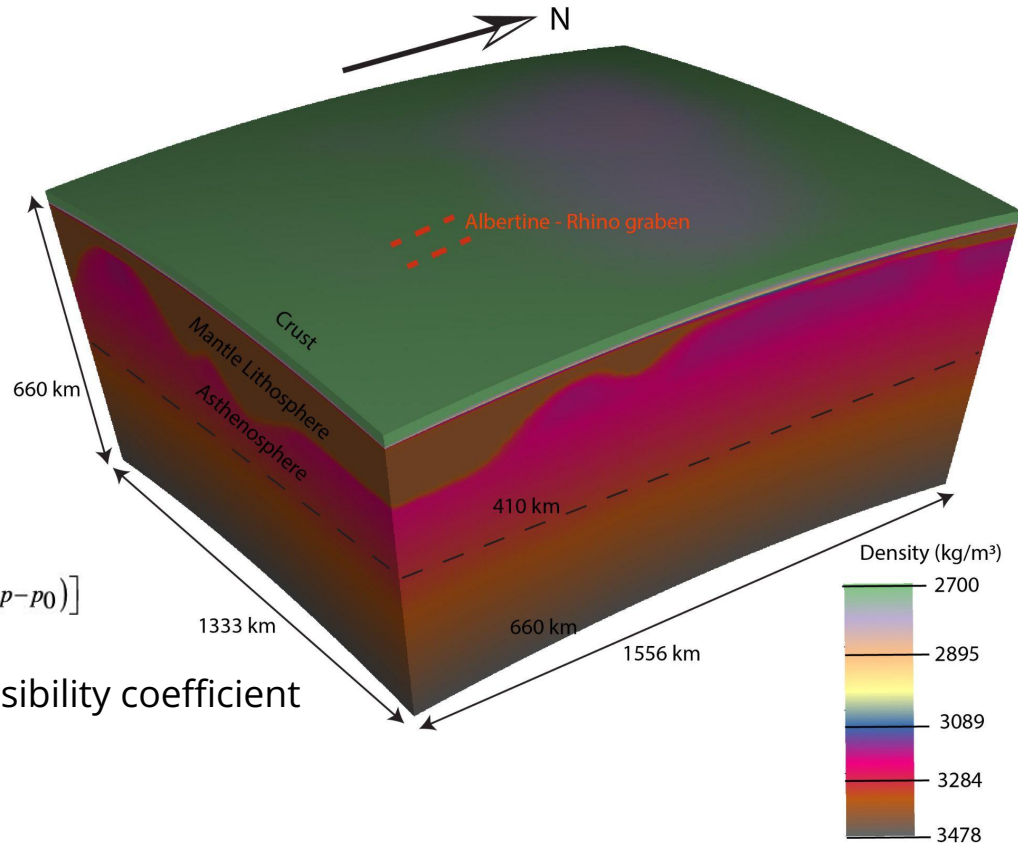
Crust - constant of 2700 kg/m^3

Mantle lithosphere - constant of 3300 kg/m^3

Below the LAB - Density is depends on temperature and pressure

$$\rho_{solid, melt} = \rho(T, p) = \rho_0 [1 - \alpha(T - T_0)] e^{\beta(p - p_0)}$$

α - thermal expansion and β is the compressibility coefficient

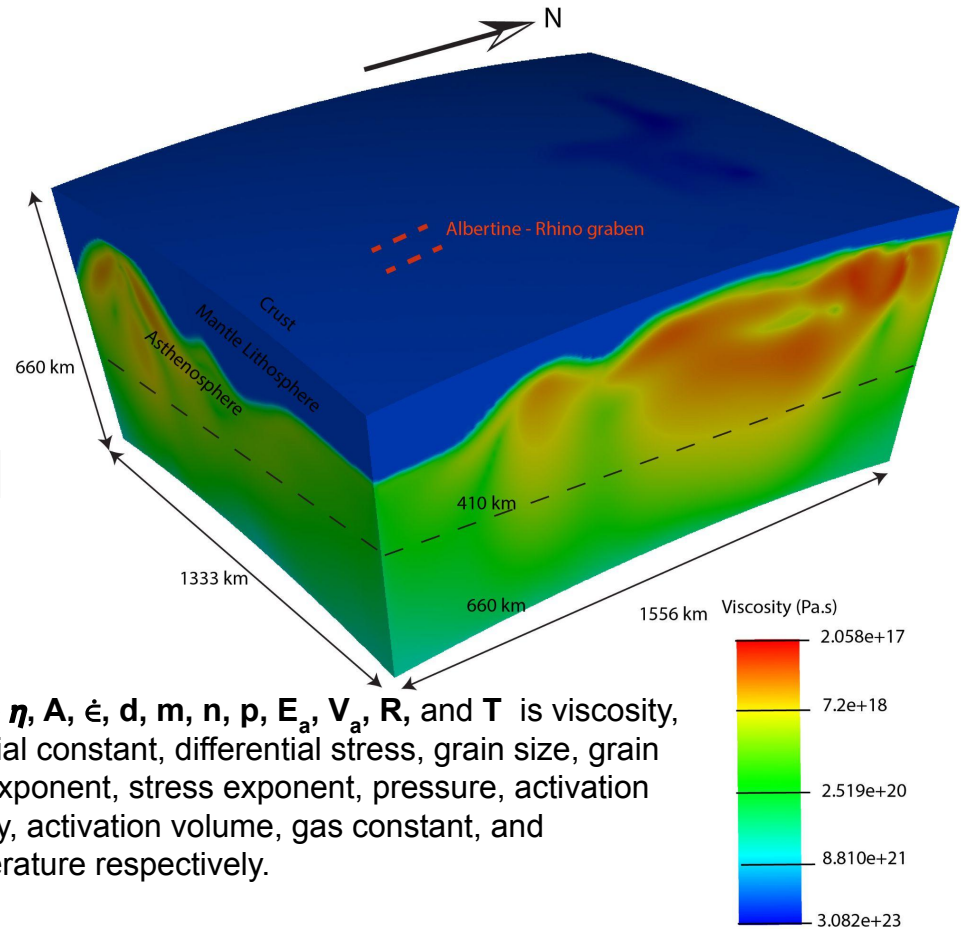


Model Set-up

Initial viscosity conditions:

Lithosphere: 10^{23} Pa.s (Lithosphere is made rigid by imposing a higher viscosity)

Below the LAB: Apply a composite rheology, which is the harmonic average of dislocation creep and diffusion creep for the viscous deformation.



$$\eta_{diff, disl} = \frac{1}{2} A^{-\frac{1}{n}} d^{\frac{m}{n}} \dot{\epsilon}^{\frac{1-n}{n}} \exp\left(\frac{E_a + pV_a}{nRT}\right)$$

$$\eta_{comp} = \frac{\eta_{diff} \times \eta_{disl}}{\eta_{diff} + \eta_{disl}}$$

where η , A , $\dot{\epsilon}$, d , m , n , p , E_a , V_a , R , and T is viscosity, material constant, differential stress, grain size, grain size exponent, stress exponent, pressure, activation energy, activation volume, gas constant, and temperature respectively.

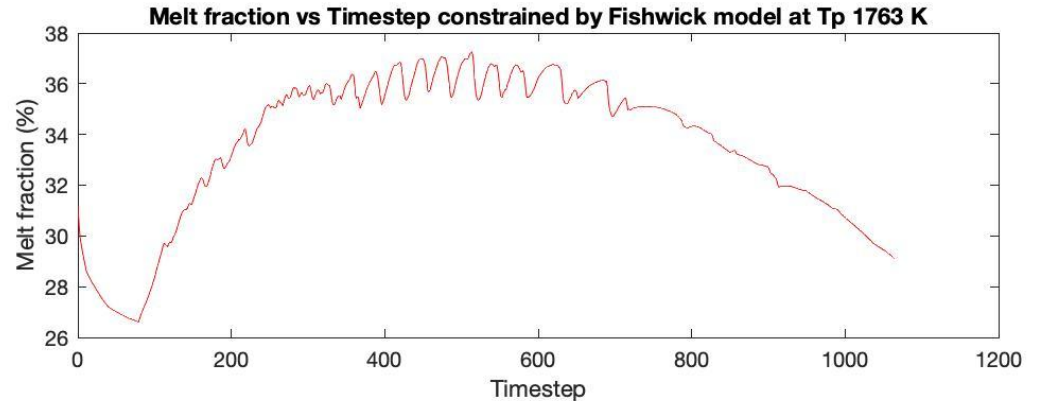
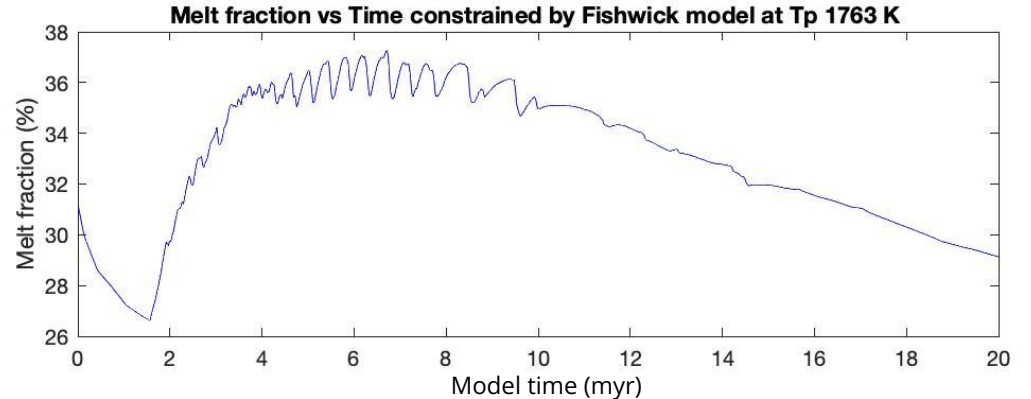
Experimentation

Information obtained from the plots

- Find at what time step the model reaches “steady-state”.
- We make the assumption that the peak of melt generation after the initial decay happens when the model reaches “steady-state”.

The peak of melt generation after the initial decay for T_p 1763 K based on Fishwick model is at time-step 500

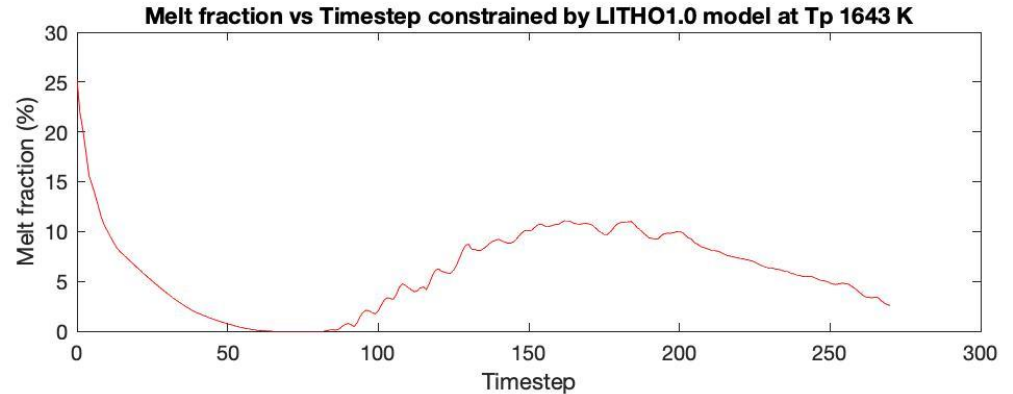
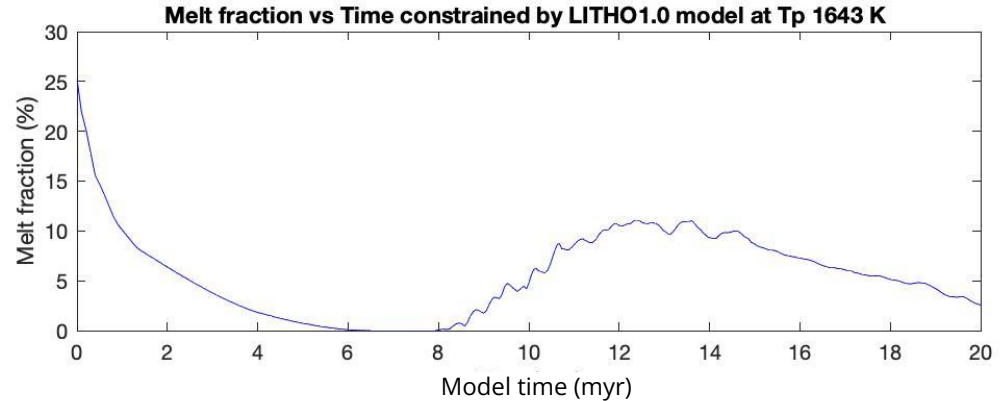
Melt fraction Vs Model time/timestep plots



Experimentation

The peak of melt generation after the initial decay for Tp 1643 K based on LITHO1.0 model is at time-step 160

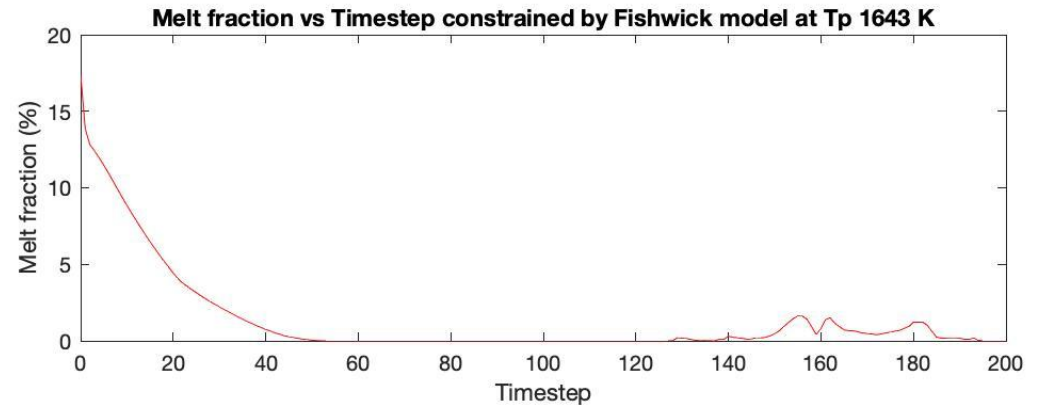
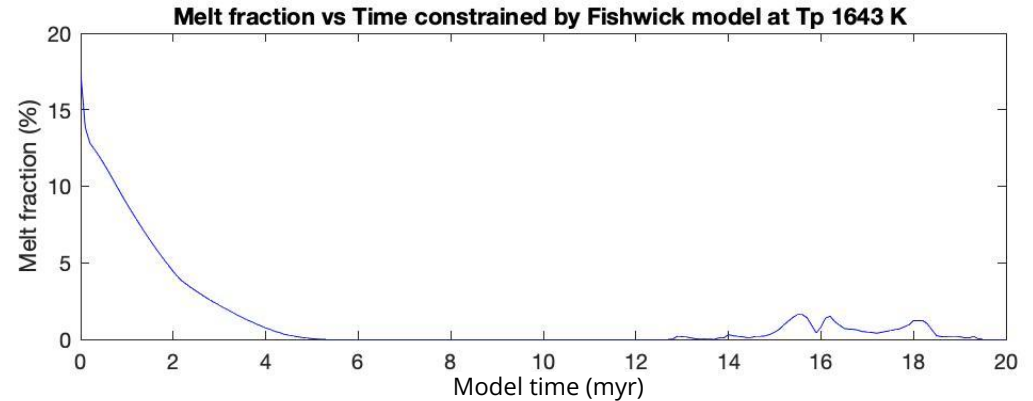
Melt fraction Vs Model time/timestep plots



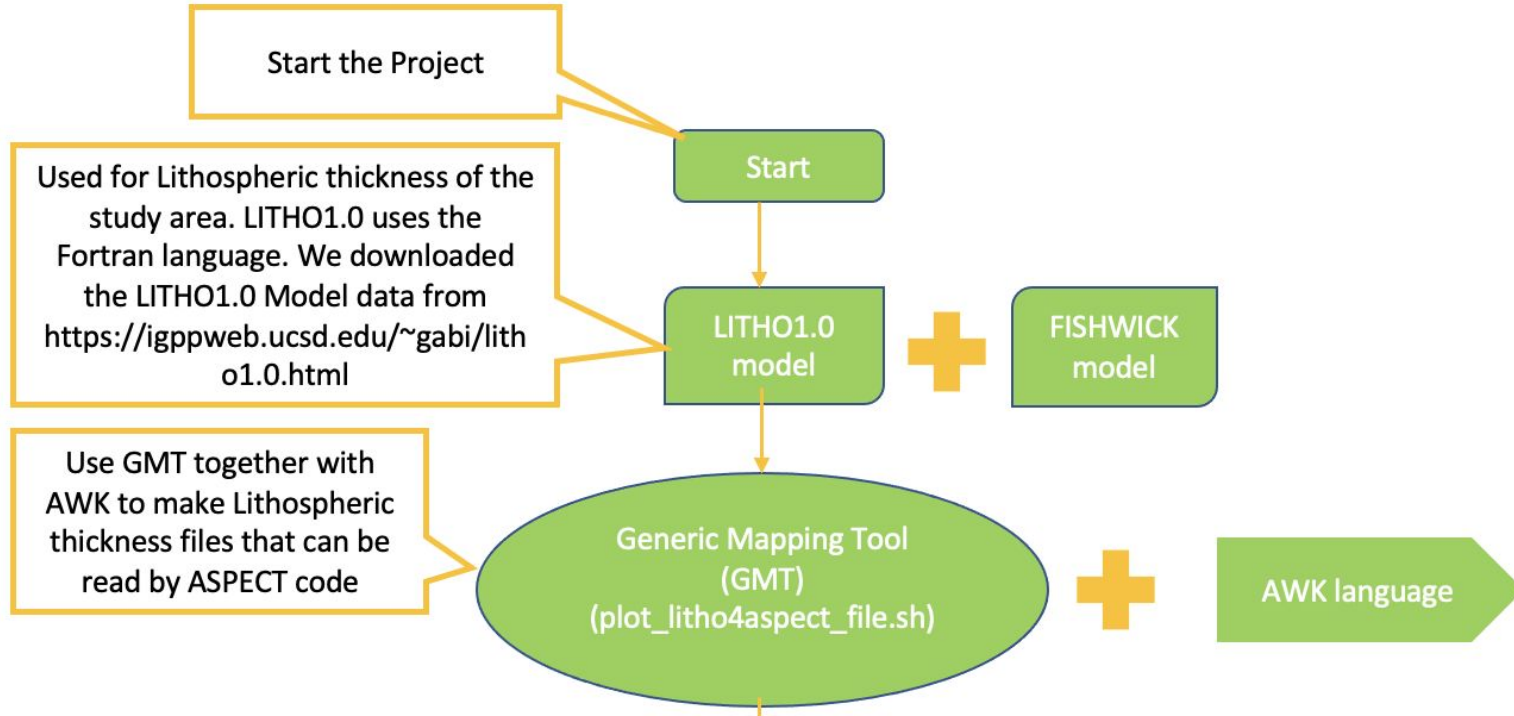
Experimentation

The highest melt fraction after the initial decay for Tp 1643 K based on Fishwick model is at time-step 155

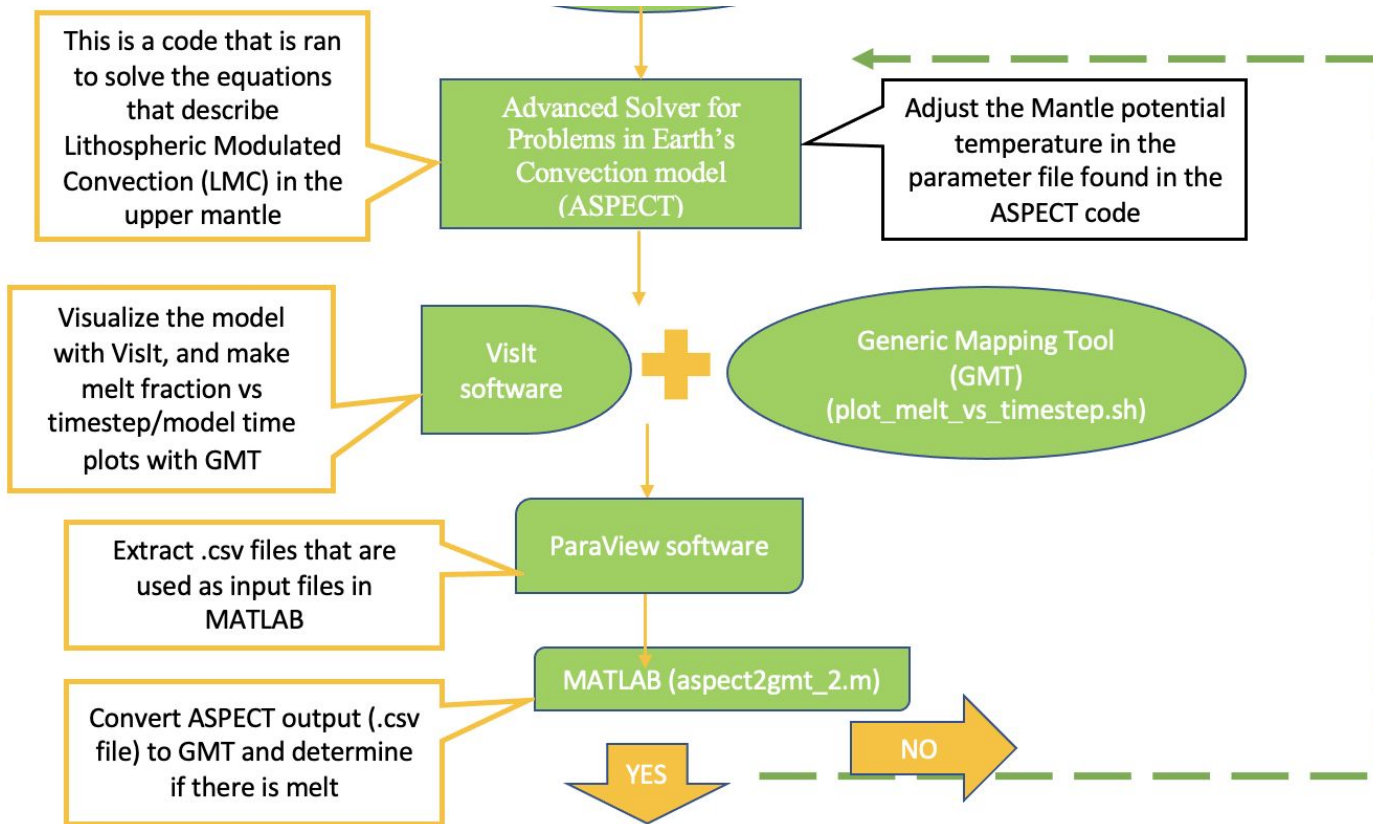
Melt fraction Vs Model time/timestep plots



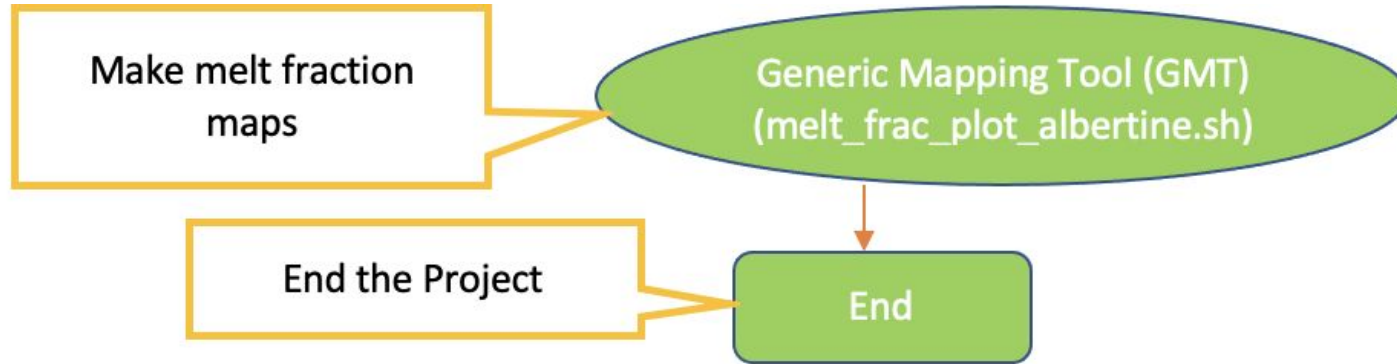
Workflow

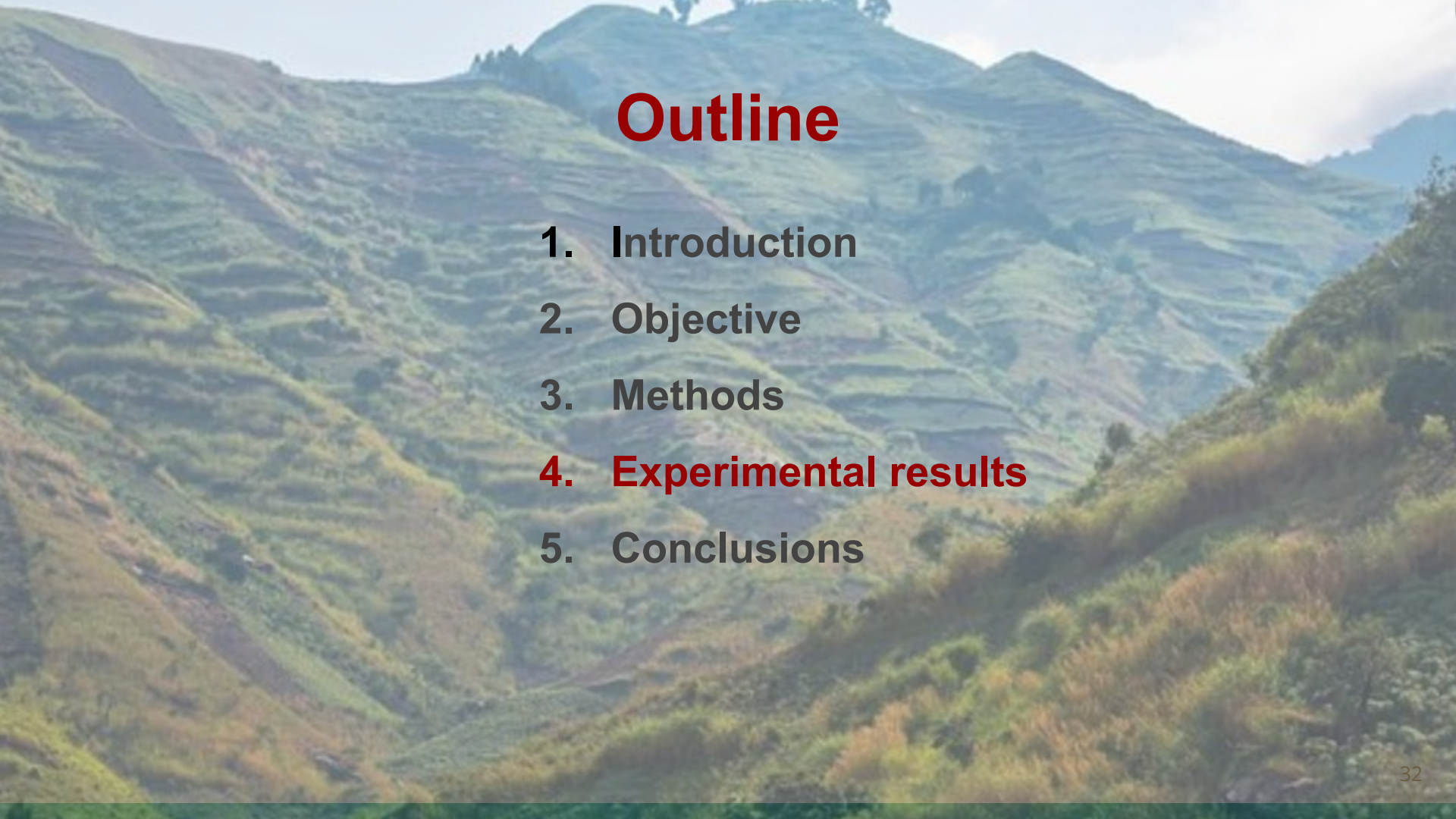


Workflow



Workflow



A scenic view of a mountain valley with terraced fields and a winding road. The landscape is lush green with some brown patches, suggesting a rural or agricultural setting. The mountains in the background are hazy and blue.

Outline

1. Introduction
2. Objective
3. Methods
4. **Experimental results**
5. Conclusions

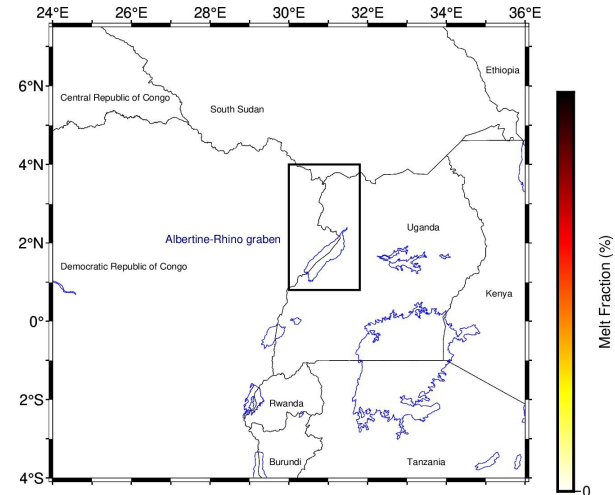
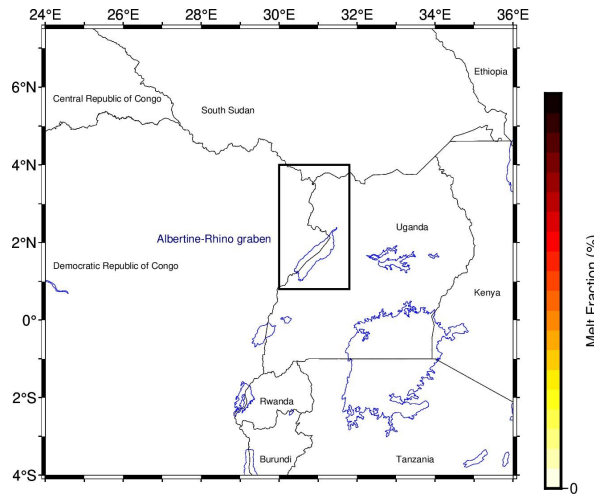
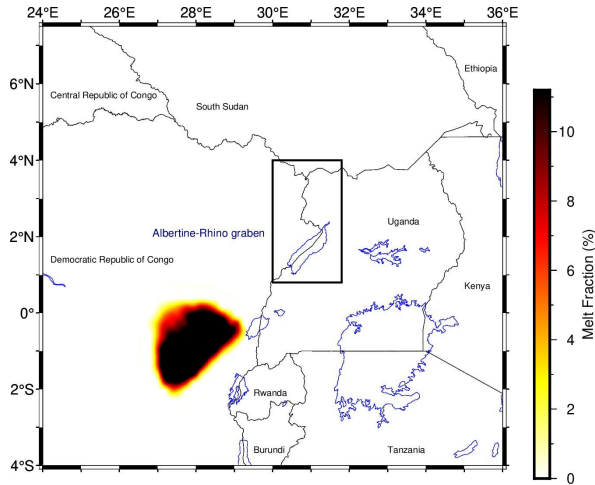
Melt Generation from LMC based on the LITHO1.0 model

LAB depth beneath Albertine-Rhino Graben based on LITHO1.0 = 60 to 220 km

$T_p = 1643$ K at 65 km depth

$T_p = 1643$ K at 145 km depth

$T_p = 1643$ K at 225 km depth



Timestep = 160
Model time = 13 Myr

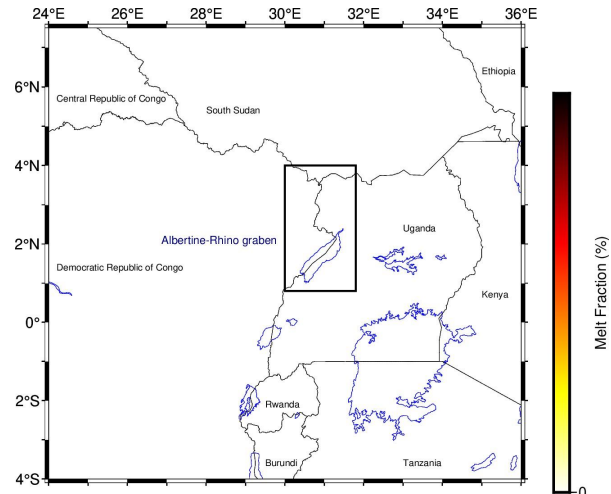
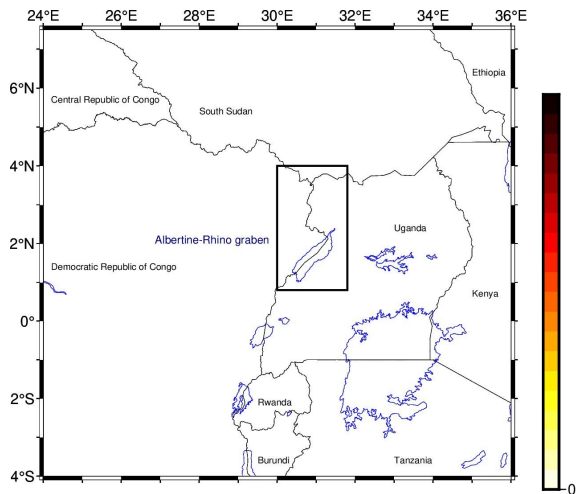
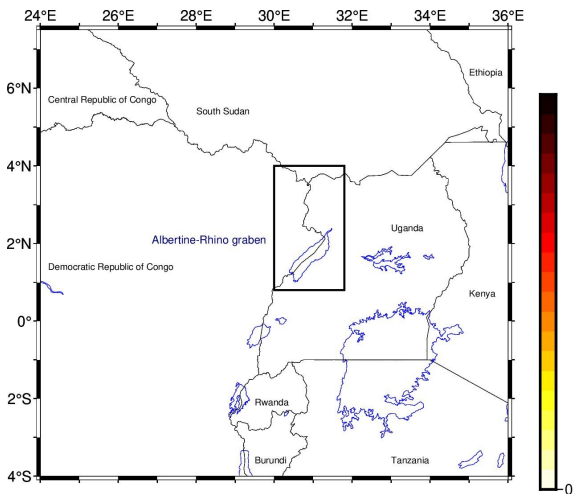
Melt Generation from LMC based on the LITHO1.0 model

LAB depth beneath Albertine-Rhino Graben based on LITHO1.0 = 60 to 220 km

$T_p = 1653$ K at 65 km depth

$T_p = 1653$ K at 145 km depth

$T_p = 1653$ K at 225 km depth



Timestep = 180
Model time = 15 Myr

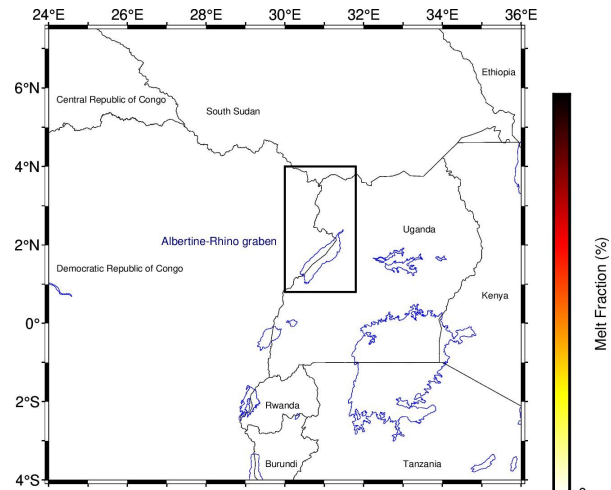
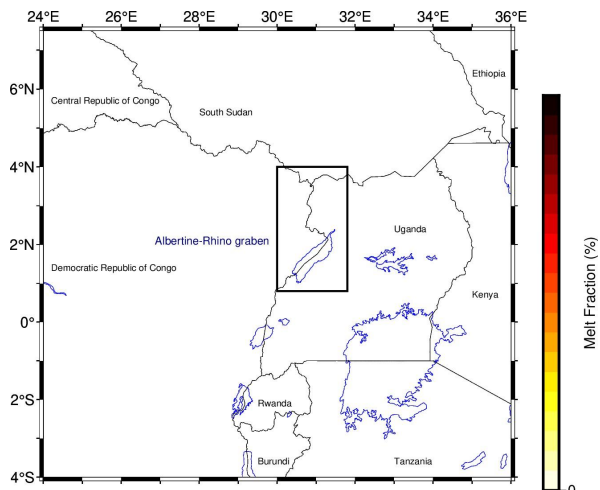
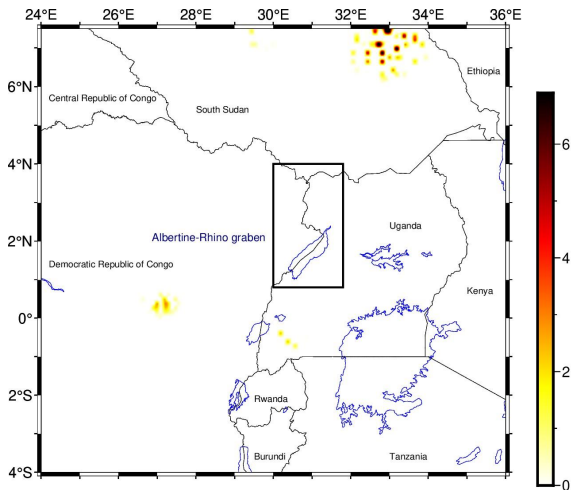
Melt Generation from LMC based on the LITHO1.0 model

LAB depth beneath Albertine-Rhino Graben based on LITHO1.0 = 60 to 220 km

$T_p = 1673$ K at 65 km depth

$T_p = 1673$ K at 145 km depth

$T_p = 1673$ K at 225 km depth



Timestep = 180
Model time = 15 Myr

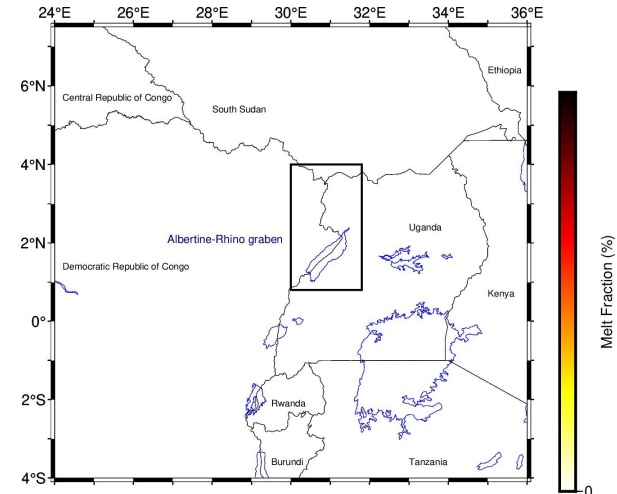
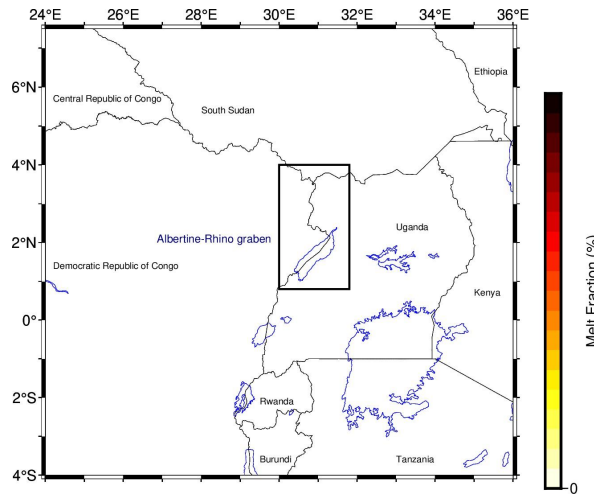
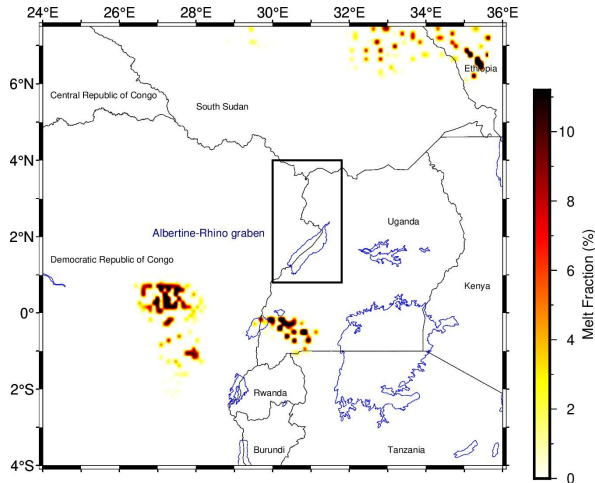
Melt Generation from LMC based on the LITHO1.0 model

LAB depth beneath Albertine-Rhino Graben based on LITHO1.0 = 60 to 220 km

$T_p = 1693$ K at 65 km depth

$T_p = 1693$ K at 145 km depth

$T_p = 1693$ K at 225 km depth

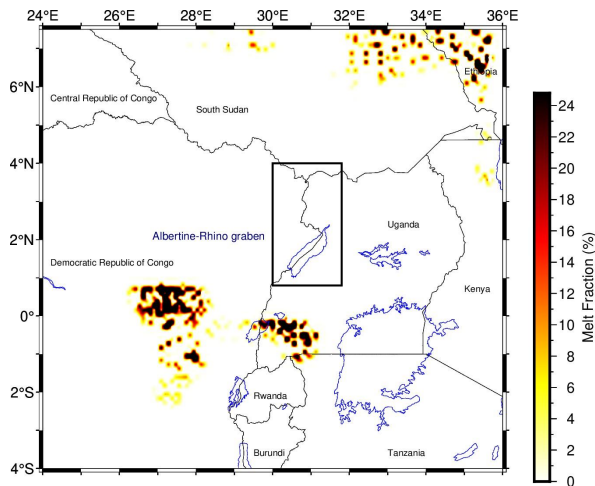


Timestep = 470
Model time = 18 Myr

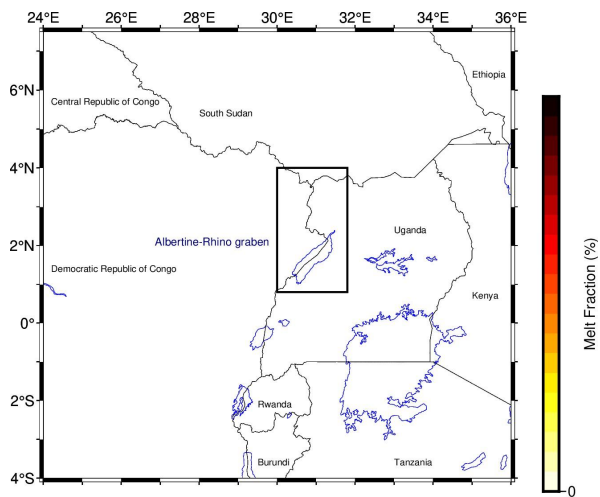
Melt Generation from LMC based on the LITHO1.0 model

LAB depth beneath Albertine-Rhino Graben based on LITHO1.0 = 60 to 220 km

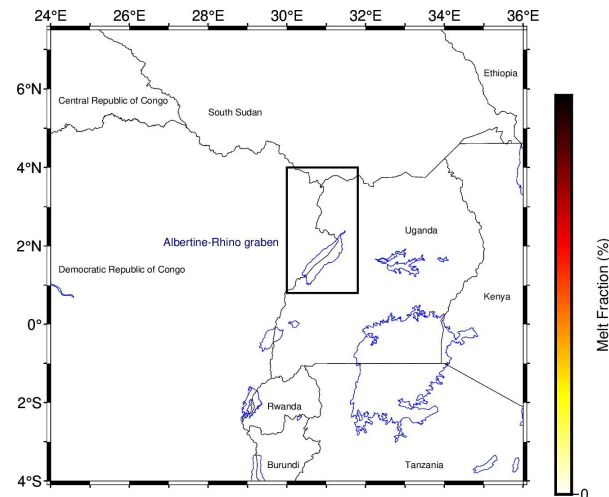
$T_p = 1700$ K at 65 km depth



$T_p = 1700$ K at 145 km depth



$T_p = 1700$ K at 225 km depth

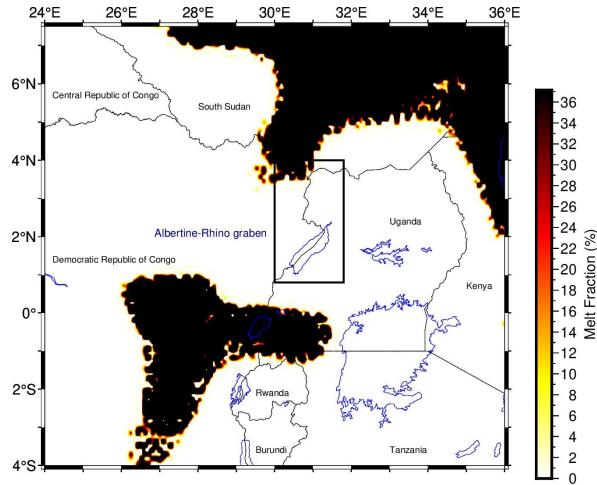


Timestep = 530
Model time = 16.6 Myr

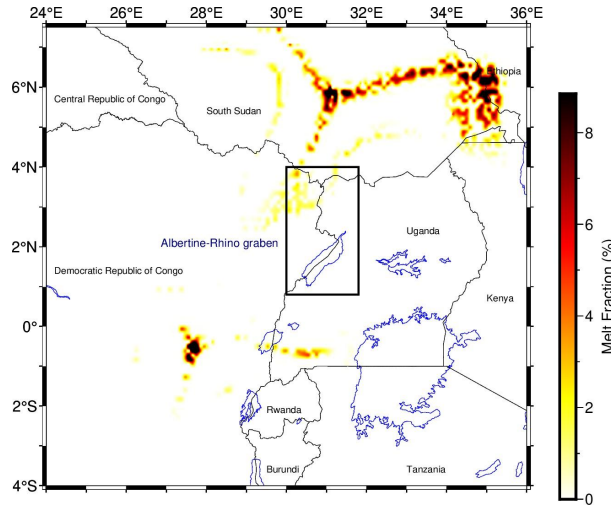
Melt Generation from LMC based on the LITHO1.0 model

LAB depth beneath Albertine-Rhino Graben based on LITHO1.0 = 60 to 220 km

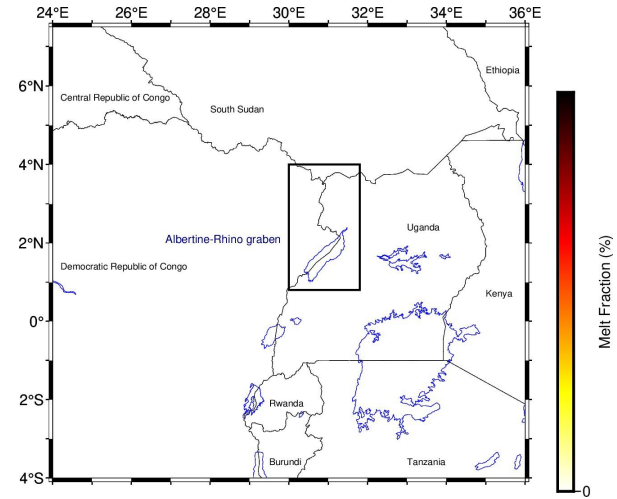
$T_p = 1763$ K at 65 km depth



$T_p = 1763$ K at 145 km depth



$T_p = 1763$ K at 225 km depth



Timestep = 350
Model time = 2.8Myr

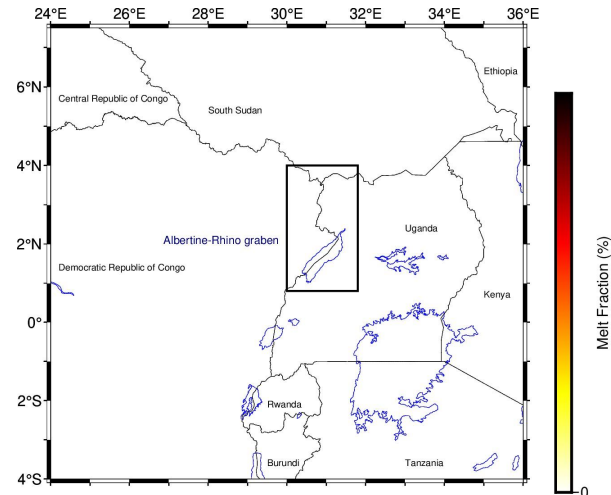
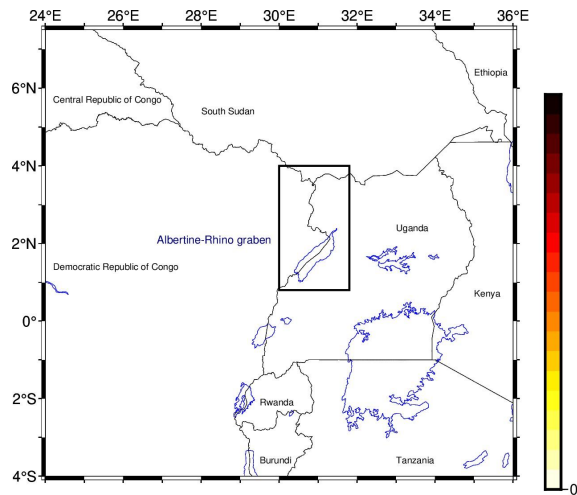
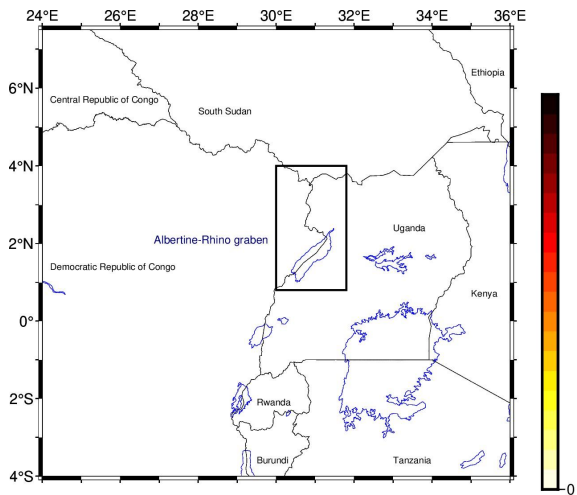
Melt Generation from LMC based on the Fishwick (2010,updated) model

LAB depth beneath Albertine-Rhino Graben based on Fishwick = 105 to 165 km

$T_p = 1643$ K at 110 km depth

$T_p = 1643$ K at 140 km depth

$T_p = 1643$ K at 170 km depth



Timestep = 155
Model time = 15.5 Myr

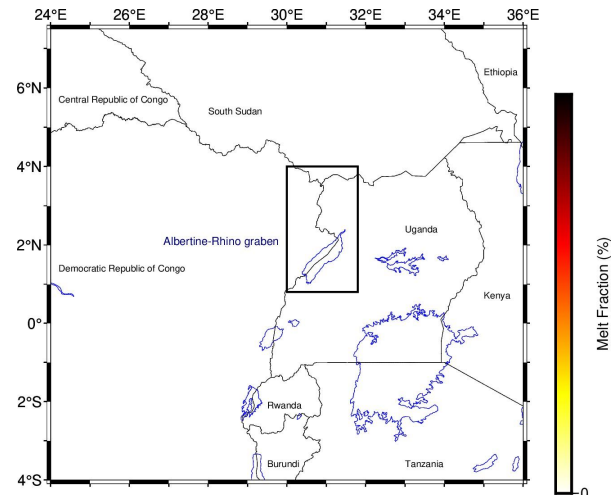
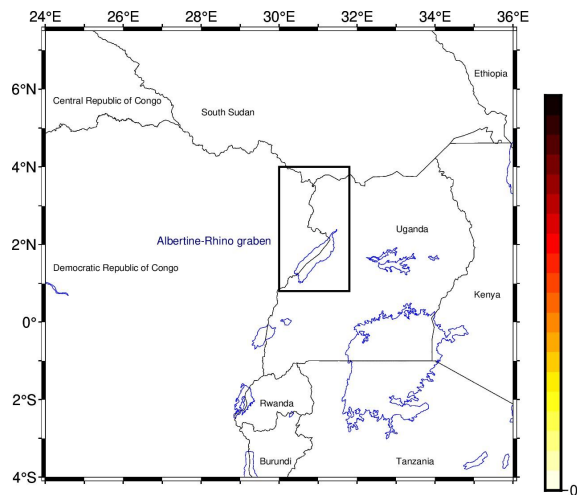
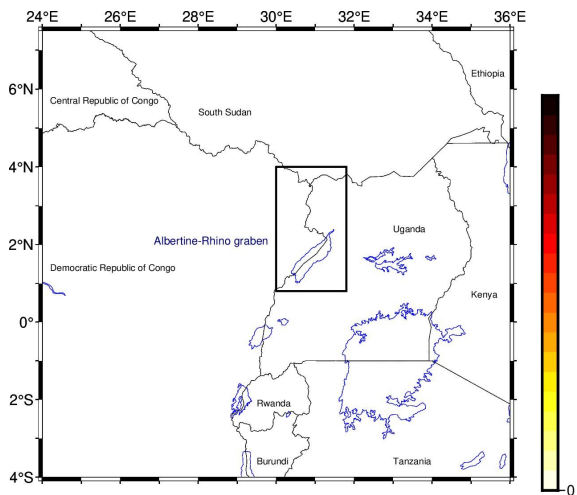
Melt Generation from LMC based on the Fishwick (2010,updated) model

LAB depth beneath Albertine-Rhino Graben based on Fishwick = 105 to 165 km

$T_p = 1653$ K at 110 km depth

$T_p = 1653$ K at 140 km depth

$T_p = 1653$ K at 170 km depth

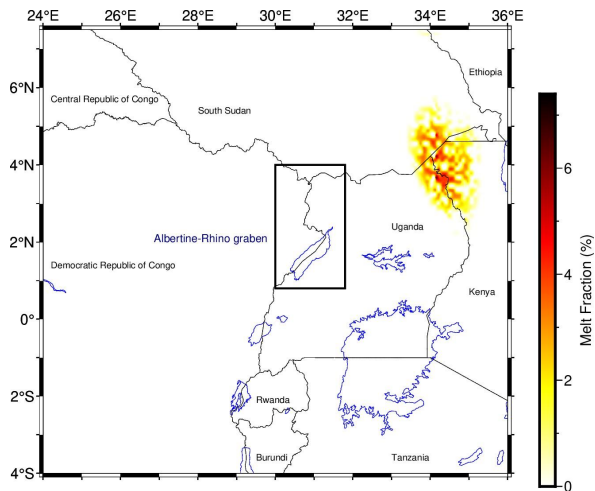


Timestep = 200
Model time = 16 Myr

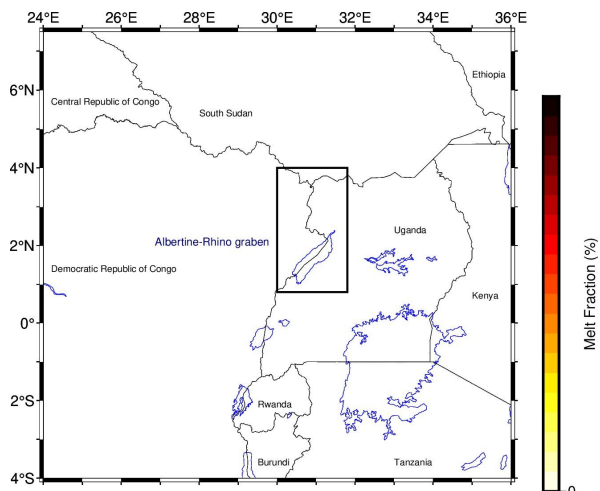
Melt Generation from LMC based on the Fishwick (2010,updated) model

LAB depth beneath Albertine-Rhino Graben based on Fishwick = 105 to 165 km

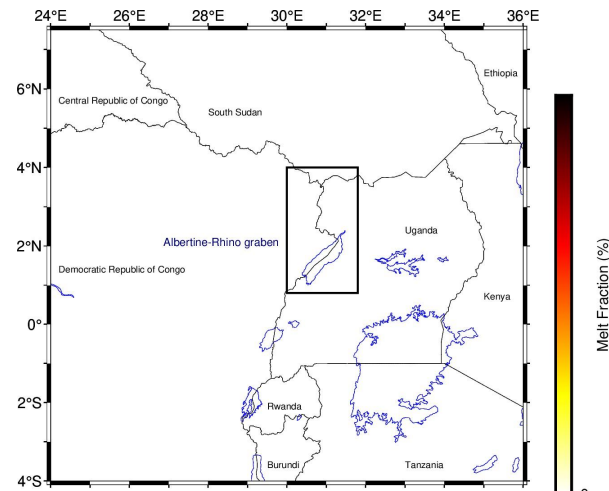
$T_p = 1673$ K at 110 km depth



$T_p = 1673$ K at 140 km depth



$T_p = 1673$ K at 170 km depth

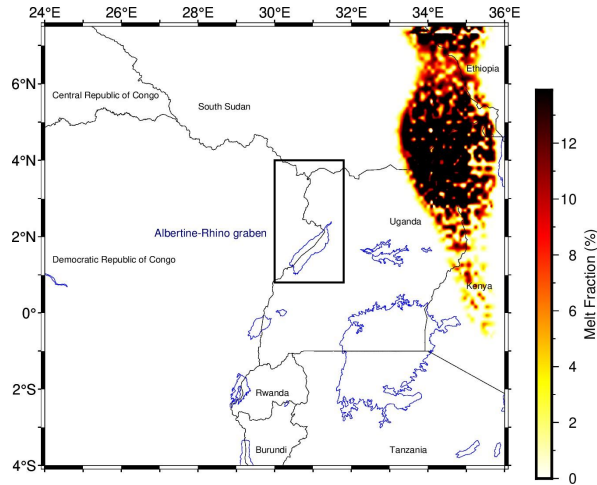


Timestep = 225
Model time = 17 Myr

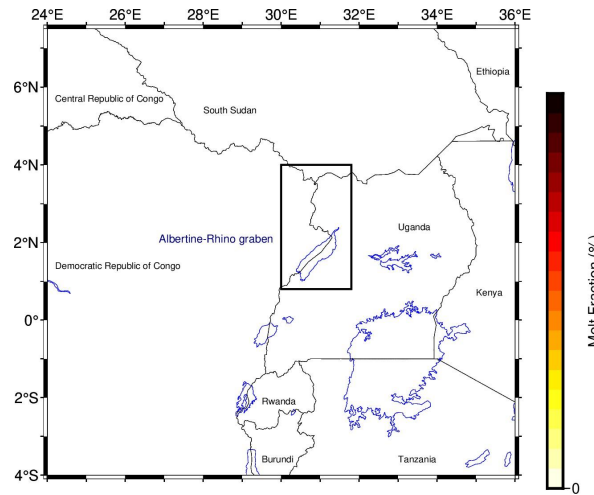
Melt Generation from LMC based on the Fishwick (2010,updated) model

LAB depth beneath Albertine-Rhino Graben based on Fishwick = 105 to 165 km

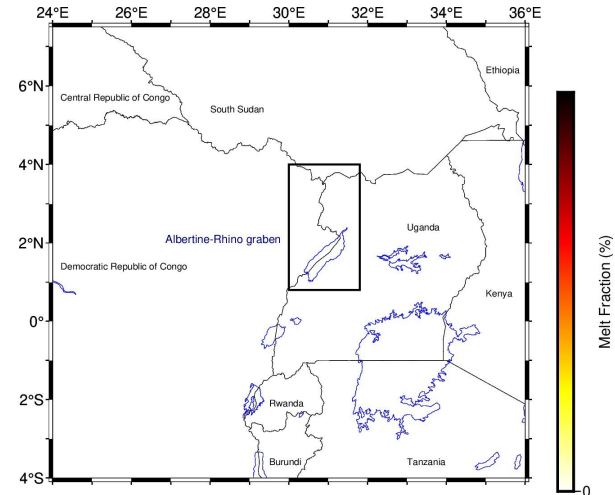
$T_p = 1693$ K at 110 km depth



$T_p = 1693$ K at 140 km depth



$T_p = 1693$ K at 170 km depth

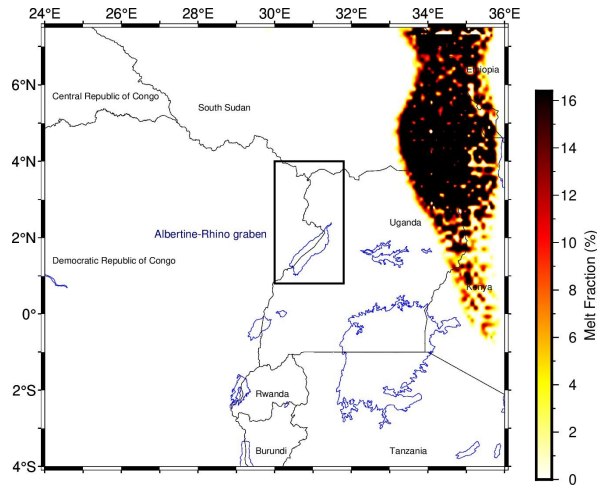


Timestep = 260
Model time = 13 Myr

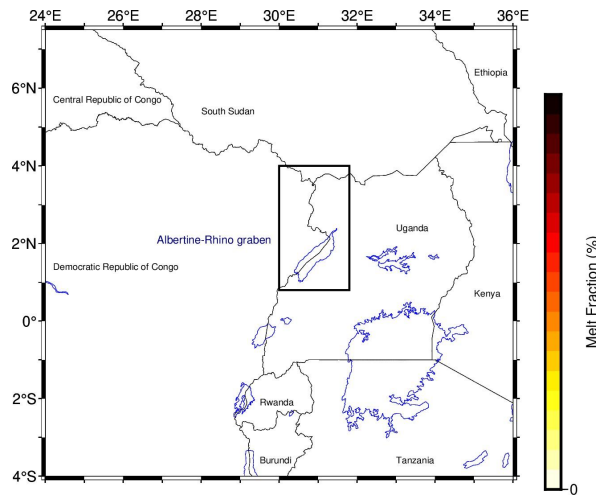
Melt Generation from LMC based on the Fishwick (2010,updated) model

LAB depth beneath Albertine-Rhino Graben based on Fishwick = 105 to 165 km

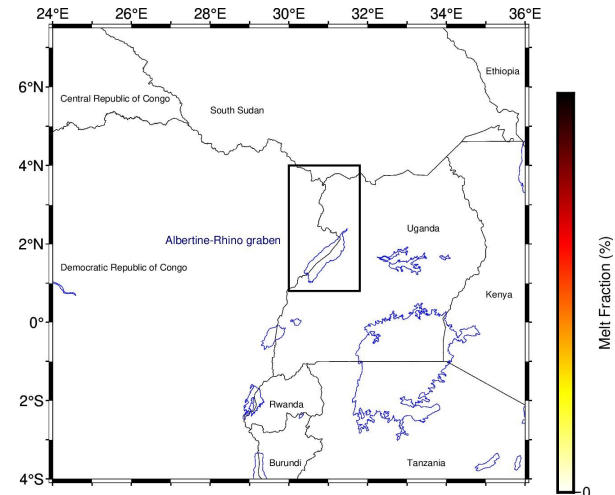
$T_p = 1700$ K at 110 km depth



$T_p = 1700$ K at 140 km depth



$T_p = 1700$ K at 170 km depth

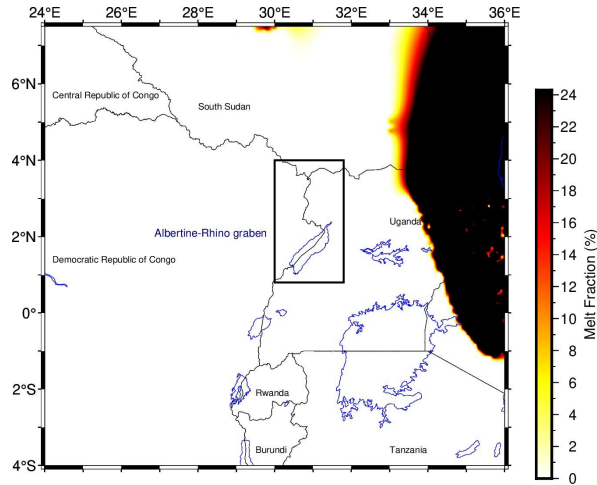


Timestep = 260
Model time = 12.2 Myr

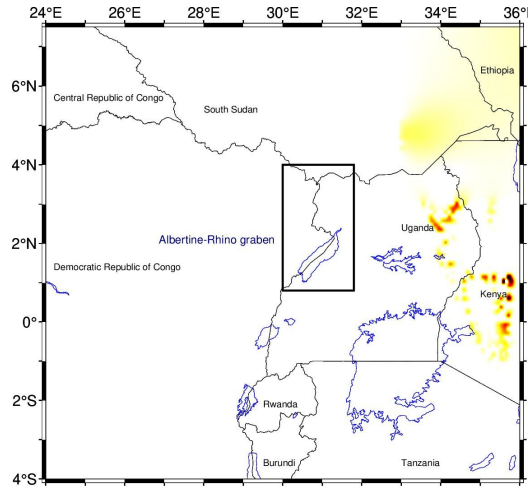
Melt Generation from LMC based on the Fishwick (2010,updated) model

LAB depth beneath Albertine-Rhino Graben based on Fishwick = 105 to 165 km

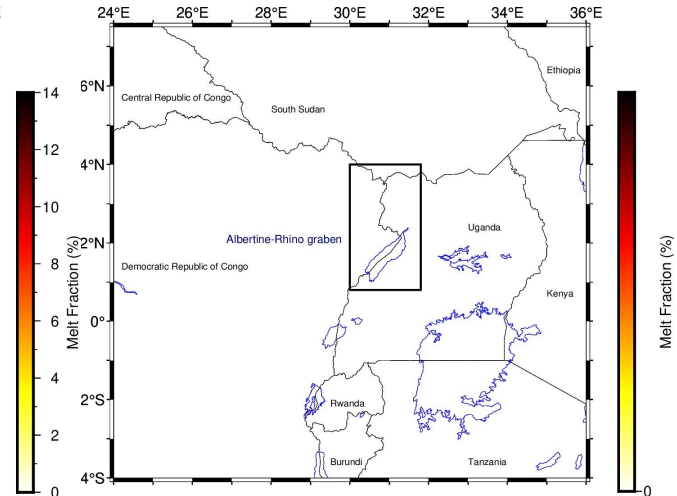
$T_p = 1763$ K at 110 km depth



$T_p = 1763$ K at 140 km depth



$T_p = 1763$ K at 170 km depth



Timestep = 500
Model time = 6.8 Myr

Outline

1. Introduction
2. Objective
3. Methods
4. Experimental results
5. **Conclusions**

- These results indicate Lithospheric Modulated Convection does not generate much melt beneath the Albertine-Rhino Graben, even with high T_p
- This implies that melt is likely not the weakening mechanism facilitating rifting of the Albertine-Rhino graben.
- The next step is to investigate the physics of pre-existing structures or fluids as weakening mechanisms that enable rifting beneath the Albertine-Rhino Graben.